

# The QCD thermal phase transition in the presence of a small chemical potential

C.R. Allton,<sup>a,b</sup> S. Ejiri,<sup>a</sup> S.J. Hands,<sup>a,c</sup> O. Kaczmarek,<sup>d</sup> F. Karsch,<sup>c,d</sup> E. Laermann,<sup>d</sup> Ch. Schmidt,<sup>d</sup> and L. Scorzato<sup>a</sup> \*

<sup>a</sup>*Department of Physics, University of Wales Swansea, Singleton Park, Swansea, SA2 8PP, U.K.*

<sup>b</sup>*Department of Mathematics, University of Queensland, Brisbane 4072, Australia*

<sup>c</sup>*Institute for Theoretical Physics, University of California, Santa Barbara, CA 93106-4030, U.S.A.*

<sup>d</sup>*Fakultät für Physik, Universität Bielefeld, D-33615 Bielefeld, Germany*

(February 8, 2020)

We propose a new method to investigate the thermal properties of QCD with a small quark chemical potential  $\mu$ . Derivatives of the phase transition point with respect to  $\mu$  are computed at  $\mu = 0$  for 2 flavors of p-4 improved staggered fermions with  $ma = 0.1, 0.2$  on a  $16^3 \times 4$  lattice. The resulting Taylor expansion is well behaved for the small values of  $\mu_q/T_c \sim 0.1$  relevant for RHIC phenomenology, and predicts a critical curve  $T_c(\mu)$  in reasonable agreement with estimates obtained using exact reweighting. In addition, we contrast the case of isoscalar and isovector chemical potentials, quantify the effect of  $\mu \neq 0$  on the equation of state, and comment on the complex phase of the fermion determinant in QCD with  $\mu \neq 0$ .

11.15.Ha, 12.38.Gc, 12.38.Mh, 05.70.Ce

## I. INTRODUCTION

The study of the phase structure of QCD at non-zero temperature and baryon density is one of the most interesting topics in contemporary physics. Heavy-ion collision experiments are running at BNL and CERN with the goal of the experimental production of a new state of matter, the quark-gluon plasma [1]. On the theoretical side, novel color superconducting and superfluid phases have been conjectured at high baryon densities [2]. For these reasons the need for numerical studies of the QCD phase transition using lattice gauge theory simulations, currently the most powerful quantitative approach to QCD, with both temperature  $T \neq 0$  and quark chemical potential  $\mu_q \neq 0$ , is more urgent than ever. Precise theoretical inputs from simulations in the vicinity of the QCD phase transition are indispensable to the understanding of the heavy-ion collision experiments.

Over the last several years, the numerical study of lattice QCD has been successful at zero chemical potential and high temperature [3]. In contrast, because the quark determinant is complex at  $\mu \neq 0$  and Monte-Carlo simulation not directly applicable, studies at non-zero  $\mu$  are still largely exploratory. Recent developments with  $\mu \neq 0$  can be classified in two categories [4]. At the low temperatures and high densities where the new phases are expected, studies of model field theories such as two-color (SU(2)) QCD and the NJL model have been made. The simulation is possible because in both cases the quark determinant is positive definite so that conventional Monte Carlo methods can be used. The other case is high temperature and low density, which is phenomenologically more important for RHIC, since the QCD phase transition both in the early universe and in the interesting regime for heavy-ion collisions is expected at rather low density, e.g.,  $\mu_q \sim 15\text{MeV}$  ( $\mu_q/T_c \sim 0.1$ ) for RHIC [5]. In this region the reweighting method, in which observables at  $\mu \neq 0$  are computed by performing simulations at  $\text{Re}(\mu) = 0$ , is applicable [6]. Using this method, the first results on the phase structure in the  $(\mu, T)$  plane were recently obtained by Fodor and Katz [7]. Unfortunately, rather general arguments suggest the region of applicability of the reweighting method becomes narrower as the lattice volume is increased. Another efficient method at low density is via a Taylor expansion obtained by computing the derivatives of physical quantities with respect to  $\mu$  at  $\mu = 0$ . This approach is not restricted to small lattices, because it requires only the expectation values of local fermion bilinears; these are measured effectively on large systems using stochastic methods, and might even be expected to self-average as the volume increases. Since analyticity is required, however, the values of  $\mu$  which can be reached must be bounded by, e.g. the critical point expected in the  $(\mu, T)$  plane for QCD with 2 light flavors. Pioneering work in such a framework have been made by developing expansions for free energy, yielding quark number susceptibility [8,9], and for hadronic screening masses [10].

---

\*Present address: DESY Theory Division, Notkestrasse 85, D-22603 Hamburg, Germany.

In this study, we investigate the transition temperature  $T_c$  as a function of  $\mu \neq 0$ . In Sec. II, we propose a new method to compute derivatives of physical quantities with respect to  $\mu$ . Details of our simulations performed on a  $16^3 \times 4$  lattice with quark masses  $m = 0.1, 0.2$  are presented in Sec. III. In Sec. IV we check the feasibility of the method by calculating the derivative of the transition point with respect to  $m$ . Our main result, the calculation of the second derivative of  $\beta_c$  with respect to  $\mu$  for 2 flavor QCD, is given in Sec. V. Using data on the lattice beta-function, we are then able to translate this result into physical units, yielding an estimate for the phase transition line  $T_c(\mu)$ . We also discuss the response of the pressure  $p(T)$  and energy density  $\epsilon(T)$  to non-zero  $\mu$ , and estimate their variation along the critical line. Finally in this section we discuss the problem of the complex phase of the quark determinant, and show that the sign problem is mild in the region of the phase diagram relevant for RHIC physics. Section VI presents our conclusions.

## II. REWEIGHTING METHOD FOR THE $\mu$ -DIRECTION

Ferrenberg and Swendsen's reweighting method is a very useful technique to investigate critical phenomena [11]. In QCD the expectation value of an observable  $\mathcal{O}(\beta, m, \mu)$  can in principle be computed by simulation at  $(\beta_0, m_0, \mu_0)$  using the following identity:

$$\langle \mathcal{O} \rangle_{(\beta, m, \mu)} = \frac{1}{Z(\beta, m, \mu)} \int \mathcal{D}U \mathcal{O}(\det M(m, \mu))^{\alpha N_f} e^{-S_g(\beta)} \quad (1)$$

$$= \frac{\langle \mathcal{O} e^{\alpha N_f (\ln \det M(m, \mu) - \ln \det M(m_0, \mu_0))} e^{-S_g(\beta) + S_g(\beta_0)} \rangle_{(\beta_0, m_0, \mu_0)}}{\langle e^{\alpha N_f (\ln \det M(m, \mu) - \ln \det M(m_0, \mu_0))} e^{-S_g(\beta) + S_g(\beta_0)} \rangle_{(\beta_0, m_0, \mu_0)}}. \quad (2)$$

Here  $M$  is the quark matrix,  $S_g$  the gauge action,  $N_f$  the number of flavors, and  $\alpha = 1$  or  $1/4$  for Wilson or staggered lattice fermions respectively. The chemical potential parameter  $\mu = \mu_q a$ , where  $a$  is the lattice spacing. Because  $\det M(\mu)$  is complex for  $\text{Re}(\mu) \neq 0$ , the expectation values in (2) can only be estimated by conventional Monte Carlo importance sampling if the simulation is performed for  $\mu_0$  zero or pure imaginary. Most of the attempts to calculate at  $\mu \neq 0$  have used variants of this method [6]. The reweighting factor for the gauge part is easy to compute by measuring the plaquette  $P_{\mu\nu}$ , since

$$-S_g(\beta) + S_g(\beta_0) = (\beta - \beta_0) \sum_{x, \mu > \nu} P_{\mu\nu}(x), \quad (3)$$

for the standard Wilson action, and extensions for improved actions are easy to derive. However, to compute the fermion part, the calculation of the fermion determinant is required for each point  $(m, \mu)$  we want to study. Such a calculation is quite expensive and difficult to perform in practice. Fodor and Katz have performed such calculations, and by reweighting in both  $\mu$  and  $\beta$  have succeeded in tracing out the critical line  $\beta_c(\mu)$  and locating the critical endpoint on small lattices [7]. Their method exploits the fact that the overlap between ensembles at different points along the coexistence line separating hadronic and quark-gluon plasma phases remains reasonably large on finite systems.

Another problem of the reweighting method is the sign problem, which will be discussed in detail later. As  $\mu$  increases from zero, the calculation of eqn.(2) becomes more difficult due to fluctuations in the phase of the denominator. To avoid these problems, we restrict ourselves to calculating derivatives of physical quantities with respect to  $\mu$ , which can be done at  $\mu = 0$ . This yields estimates of the physical quantity as a continuous function of  $\mu$  in a narrow range of  $\mu$ , but the region of applicability is not restricted to the immediate neighbourhood of the phase transition. The Taylor expansion in  $\mu^1$  for the fermionic part of the reweighting factor around  $\mu = 0$  is

$$\alpha N_f \ln \left( \frac{\det M(\mu)}{\det M(0)} \right) = \alpha N_f \sum_{n=1}^{\infty} \frac{\mu^n}{n!} \frac{\partial^n \ln \det M(0)}{\partial \mu^n} \equiv \sum_{n=1}^{\infty} \mathcal{R}_n \mu^n. \quad (4)$$

We similarly expand fermionic observables such as the chiral condensate,

$$\langle \bar{\psi} \psi \rangle = (N_s^3 \times N_t)^{-1} \alpha N_f \langle \text{tr} M^{-1} \rangle, \quad (5)$$

---

<sup>1</sup>Strictly speaking this is an expansion in  $\mu_q/T$  for fixed  $T$ , ie. a fugacity expansion.

where the lattice size is  $N_s^3 \times N_t$ , once again obtaining a continuous function for small  $\mu$ . Using the formula

$$\frac{\partial M^{-1}}{\partial x} = -M^{-1} \frac{\partial M}{\partial x} M^{-1}, \quad (6)$$

expressions for  $\partial^n(\ln \det M)/\partial \mu^n$  and  $\partial^n(\text{tr} M^{-1})/\partial \mu^n$  in terms of traces over products of local operators and inverse matrices can be developed:

$$\begin{aligned} \frac{\partial \ln \det M}{\partial \mu} &= \text{tr} \left( M^{-1} \frac{\partial M}{\partial \mu} \right), \\ \frac{\partial^2 \ln \det M}{\partial \mu^2} &= \text{tr} \left( M^{-1} \frac{\partial^2 M}{\partial \mu^2} \right) - \text{tr} \left( M^{-1} \frac{\partial M}{\partial \mu} M^{-1} \frac{\partial M}{\partial \mu} \right), \\ \frac{\partial^3 \ln \det M}{\partial \mu^3} &= \text{tr} \left( M^{-1} \frac{\partial^3 M}{\partial \mu^3} \right) - 3\text{tr} \left( M^{-1} \frac{\partial M}{\partial \mu} M^{-1} \frac{\partial^2 M}{\partial \mu^2} \right) + 2\text{tr} \left( M^{-1} \frac{\partial M}{\partial \mu} M^{-1} \frac{\partial M}{\partial \mu} M^{-1} \frac{\partial M}{\partial \mu} \right), \end{aligned} \quad (7)$$

$$\begin{aligned} \frac{\partial \text{tr} M^{-1}}{\partial \mu} &= -\text{tr} \left( M^{-1} \frac{\partial M}{\partial \mu} M^{-1} \right), \\ \frac{\partial^2 \text{tr} M^{-1}}{\partial \mu^2} &= -\text{tr} \left( M^{-1} \frac{\partial^2 M}{\partial \mu^2} M^{-1} \right) + 2\text{tr} \left( M^{-1} \frac{\partial M}{\partial \mu} M^{-1} \frac{\partial M}{\partial \mu} M^{-1} \right), \\ \frac{\partial^3 \text{tr} M^{-1}}{\partial \mu^3} &= -\text{tr} \left( M^{-1} \frac{\partial^3 M}{\partial \mu^3} M^{-1} \right) + 3\text{tr} \left( M^{-1} \frac{\partial^2 M}{\partial \mu^2} M^{-1} \frac{\partial M}{\partial \mu} M^{-1} \right), \\ &\quad + 3\text{tr} \left( M^{-1} \frac{\partial M}{\partial \mu} M^{-1} \frac{\partial^2 M}{\partial \mu^2} M^{-1} \right) - 6\text{tr} \left( M^{-1} \frac{\partial M}{\partial \mu} M^{-1} \frac{\partial M}{\partial \mu} M^{-1} \frac{\partial M}{\partial \mu} M^{-1} \right). \end{aligned} \quad (8)$$

We apply the random noise method to calculate the derivatives of  $\ln \det M$  and  $\text{tr} M^{-1}$ , which enables us to compute on rather large volumes in comparison with usual studies of QCD with  $\mu \neq 0$ . Using  $N_n$  sets of random noise vectors  $\eta_{ai}$  which satisfy the condition:  $\lim_{N_n \rightarrow \infty} (1/N_n) \sum_{a=1}^{N_n} \eta_{ai}^* \eta_{aj} = \delta_{ij}$ , we rewrite the trace of products of  $\partial M/\partial \mu$  and  $M^{-1}$  as

$$\text{tr} \left( \frac{\partial^{n_1} M}{\partial \mu^{n_1}} M^{-1} \frac{\partial^{n_2} M}{\partial \mu^{n_2}} \cdots M^{-1} \right) = \lim_{N_n \rightarrow \infty} \frac{1}{N_n} \sum_{a=1}^{N_n} \eta_a^\dagger \frac{\partial^{n_1} M}{\partial \mu^{n_1}} M^{-1} \frac{\partial^{n_2} M}{\partial \mu^{n_2}} \cdots M^{-1} \eta_a. \quad (9)$$

$M^{-1} \eta_a \equiv x$  and  $M^{-1}(\partial M/\partial \mu) \cdots \eta_a \equiv x$  are obtained by solving  $Mx = \eta_a$  or  $Mx = (\partial M/\partial \mu) \cdots \eta_a$ , and we compute the RHS of eqn.(9) with finite  $N_n$ . The error for estimates of physical observables made from  $N_{\text{conf}}$  configurations is expected to decrease as  $(N_n N_{\text{conf}})^{-1/2}$ . Further notes on the application of the noise method are given in the Appendix.

By using the derivatives of both the reweighting factor and fermionic observable up to  $n$ -th order in  $\mu$ , we can obtain the correct answer for the expectation value up to  $n$ -th order, which can be easily checked by performing a Taylor expansion of the expectation value, eqn.(1), directly for each physical observable. Of course, for a pure gluonic observable such as the Polyakov loop  $L$  only the expansion of  $\ln \det M$  is needed. Furthermore, we should note that at  $\mu = 0$  the odd order derivatives of both  $\ln \det M$  and  $\text{tr} M^{-1}$  are pure imaginary and the even order derivatives are real. This property is proved using the identities for the fermion matrix:

$$M^\dagger(\mu) = \Gamma_5 M(-\mu) \Gamma_5, \quad \text{and} \quad \frac{\partial^n M^\dagger}{\partial \mu^n}(\mu) = (-1)^n \Gamma_5 \frac{\partial^n M}{\partial \mu^n}(-\mu) \Gamma_5, \quad (10)$$

where  $\Gamma_5$  is  $\gamma_5$  for Wilson fermions and  $(-1)^{x_1+x_2+x_3+x_4}$  for staggered. Then, at  $\mu = 0$

$$\text{tr} \left( M^{-1} \frac{\partial^{n_1} M}{\partial \mu^{n_1}} M^{-1} \frac{\partial^{n_2} M}{\partial \mu^{n_2}} \cdots M^{-1} \right)^* = (-1)^{n_1+n_2+\cdots} \text{tr} \left( M^{-1} \frac{\partial^{n_1} M}{\partial \mu^{n_1}} M^{-1} \frac{\partial^{n_2} M}{\partial \mu^{n_2}} \cdots M^{-1} \right). \quad (11)$$

Because the terms in the  $n$ -th derivative satisfy  $n_1 + n_2 + \cdots = n$ , we obtain

$$\left( \frac{\partial^n \ln \det M}{\partial \mu^n} \right)^* = (-1)^n \frac{\partial^n \ln \det M}{\partial \mu^n}; \quad (12)$$

$$\left( \frac{\partial^n \text{tr} M^{-1}}{\partial \mu^n} \right)^* = (-1)^n \frac{\partial^n \text{tr} M^{-1}}{\partial \mu^n}. \quad (13)$$

Using this property and the fact that  $\mathcal{Z}$  is a real function of  $\beta$ ,  $m$  and  $\mu$ , we can explicitly confirm that, if the operator has the property such that even order derivatives are real and odd order derivatives are pure imaginary at  $\mu = 0$ , e.g.,  $\langle \bar{\psi} \psi \rangle$  or its susceptibility, then all odd order derivatives of the expectation value of a physical quantity are zero at  $\mu = 0$ , as we expect from the symmetry under changing  $\mu$  to  $-\mu$ . The derivative of the expectation value can be written as a sum of products of expectation values composed of the operator, the reweighting factor and their derivatives, and the total number of differentiations in each term has to be odd for an odd order derivative. Hence all terms for odd derivatives contain at least one expectation value of a pure imaginary operator and hence vanish, since the expectation value of a pure imaginary operator is zero. Therefore the first non-trivial order of corrections to e.g.  $\langle \bar{\psi} \psi \rangle$  or its susceptibility, which we compute in this study is  $O(\mu^2)$ ; the truncation errors, so far unquantified, are  $O(\mu^4)$ .

In order to be more specific, let us define the Taylor expansion of an operator by  $\sum_{n=0}^{\infty} \mathcal{O}_n \mu^n$ . Then to  $O(\mu^2)$  the expression (2) for  $\langle \mathcal{O} \rangle_{(\beta, \mu)}$  can be rewritten

$$\langle \mathcal{O} \rangle_{(\beta, \mu)} = \frac{\langle (\mathcal{O}_0 + \mathcal{O}_1 \mu + \mathcal{O}_2 \mu^2) \exp(\mathcal{R}_1 \mu + \mathcal{R}_2 \mu^2 - \Delta S_g) \rangle}{\langle \exp(\mathcal{R}_1 \mu + \mathcal{R}_2 \mu^2 - \Delta S_g) \rangle}, \quad (14)$$

where expectation values on the RHS are measured with respect to an ensemble generated at  $(\beta_0, 0)$ . Extension of this formula to combining data from several ensembles using multi-histogramming is straightforward [11]. Further details on the evaluation of (14) using the noise method for fermionic operators are given in the Appendix.

In order to determine the pseudocritical point, we calculate the Polyakov loop susceptibility,

$$\chi_L = N_s^3 (\langle L^2 \rangle - \langle L \rangle^2), \quad (15)$$

where the Polyakov loop  $L = (N_s^3)^{-1} \sum_{\vec{x}} N_c^{-1} \text{tr} \prod_t U_4(\vec{x}, t)$ , and the susceptibility of the chiral condensate<sup>2</sup>,

$$\chi_{\bar{\psi} \psi} = (N_s^3 \times N_t)^{-1} (\alpha N_f)^2 (\langle (\text{tr} M^{-1})^2 \rangle - \langle \text{tr} M^{-1} \rangle^2). \quad (16)$$

We define the transition point  $\beta_c(\mu)$  by the peak position of these susceptibilities for each  $\mu$ ;

$$\frac{\partial \chi(\beta_c, \mu)}{\partial \beta} = 0. \quad (17)$$

If we compute  $\partial \chi / \partial \beta$  correctly up to  $n$ -th order in  $\mu$ , we can determine the  $n$ -th derivative of  $\beta_c$  with respect to  $\mu$ . For example if we determine  $\beta_c(\mu)$  using an operator such as  $\langle \bar{\psi} \psi \rangle$ , which is real and whose first derivative at  $\mu=0$  is pure imaginary, then the first derivative  $\beta'_c(\mu)$  vanishes because as argued above the first derivative of the susceptibility is zero in this case.

Finally, note we can also estimate the magnitude of fluctuations of the phase of  $\det M$ , because on each configuration this phase can be expressed in terms of the odd terms of the Taylor expansion of  $\ln \det M$ ; this will be discussed in more detail in section V C.

### III. SIMULATIONS FOR $N_F = 2$ IMPROVED STAGGERED FERMIONS

We employ a combination of the Symanzik improved gauge and 2 flavors of the p4-improved staggered fermion actions [12–14]. The partition function is defined by

$$\mathcal{Z}(\beta, m, \mu) = \int \mathcal{D}U (\det M)^{N_f/4} e^{-S_g}, \quad (18)$$

$$S_g = -\beta \left\{ \sum_{x, \mu > \nu} c_0 W_{\mu\nu}^{1 \times 1}(x) + \sum_{x, \mu, \nu} c_1 W_{\mu\nu}^{1 \times 2}(x) \right\}, \quad (19)$$

$$M_{x,y} = \sum_i \eta_i(x) \left\{ c_1^F \left[ U_i^{\text{fat}}(x) \delta_{x+\hat{i}, y} - U_i^{\text{fat}\dagger}(x - \hat{i}) \delta_{x-\hat{i}, y} \right] \right\}$$

---

<sup>2</sup> Note that we only calculate the disconnected part of the complete chiral susceptibility.

$$\begin{aligned}
& + c_3^F \sum_{i \neq j} \left[ U_{i,j}^{(1,2)}(x) \delta_{x+\hat{i}+2\hat{j},y} - U_{i,j}^{(1,2)\dagger}(x - \hat{i} - 2\hat{j}) \delta_{x-\hat{i}-2\hat{j},y} \right. \\
& + U_{i,j}^{(1,-2)}(x) \delta_{x+\hat{i}-2\hat{j},y} - U_{i,j}^{(1,-2)\dagger}(x - \hat{i} + 2\hat{j}) \delta_{x-\hat{i}+2\hat{j},y} \left. \right] \\
& + c_3^F \left[ e^{2\mu} U_{i,4}^{(1,2)}(x) \delta_{x+\hat{i}+2\hat{4},y} - e^{-2\mu} U_{i,4}^{(1,2)\dagger}(x - \hat{i} - 2\hat{4}) \delta_{x-\hat{i}-2\hat{4},y} \right. \\
& + e^{-2\mu} U_{i,4}^{(1,-2)}(x) \delta_{x+\hat{i}-2\hat{4},y} - e^{2\mu} U_{i,4}^{(1,-2)\dagger}(x - \hat{i} + 2\hat{4}) \delta_{x-\hat{i}+2\hat{4},y} \left. \right] \Big\} \\
& + \eta_4(x) \left\{ c_1^F \left[ e^\mu U_4^{\text{fat}}(x) \delta_{x+\hat{4},y} - e^{-\mu} U_4^{\text{fat}\dagger}(x - \hat{4}) \delta_{x-\hat{4},y} \right] \right. \\
& + c_3^F \sum_i \left[ e^\mu U_{4,i}^{(1,2)}(x) \delta_{x+\hat{4}+2\hat{i},y} - e^{-\mu} U_{4,i}^{(1,2)\dagger}(x - \hat{4} - 2\hat{i}) \delta_{x-\hat{4}-2\hat{i},y} \right. \\
& \left. \left. + e^\mu U_{4,i}^{(1,-2)}(x) \delta_{x+\hat{4}-2\hat{i},y} - e^{-\mu} U_{4,i}^{(1,-2)\dagger}(x - \hat{4} + 2\hat{i}) \delta_{x-\hat{4}+2\hat{i},y} \right] \right\} + m \delta_{x,y}, \quad (20)
\end{aligned}$$

where  $W_{\mu\nu}^{1\times 1}(x)$  and  $W_{\mu\nu}^{1\times 2}(x)$  are  $1\times 1$  and  $1\times 2$  Wilson loops,  $\eta_\mu(x) = (-1)^{x_1+\dots+x_{\mu-1}}$  is the KS phase and

$$\begin{aligned}
U_{\mu,\nu}^{(1,2)}(x) &= \frac{1}{2} [U_\mu(x)U_\nu(x+\hat{\mu})U_\nu(x+\hat{\mu}+\hat{\nu}) + U_\nu(x)U_\nu(x+\hat{\nu})U_\mu(x+2\hat{\nu})] , \\
U_{\mu,\nu}^{(1,-2)}(x) &= \frac{1}{2} [U_\mu(x)U_\nu^\dagger(x+\hat{\mu}-\hat{\nu})U_\nu^\dagger(x+\hat{\mu}-2\hat{\nu}) + U_\nu^\dagger(x-\hat{\nu})U_\nu^\dagger(x-2\hat{\nu})U_\mu(x-2\hat{\nu})] , \\
U_\mu^{\text{fat}}(x) &= \frac{1}{1+6\omega} \left\{ U_\mu(x) + \omega \sum_{\nu \neq \mu} [U_\nu(x)U_\mu(x+\hat{\nu})U_\nu^\dagger(x+\hat{\mu}) + U_\nu^\dagger(x-\hat{\nu})U_\mu(x-\hat{\nu})U_\nu(x+\hat{\mu}-\hat{\nu})] \right\}.
\end{aligned} \quad (21)$$

The coefficients are  $\beta = 6/g^2$ ,  $c_1 = -1/12$ ,  $c_0 = 1 - 8c_1$ ,  $c_1^F = 3/8$ ,  $c_3^F = 1/96$ , and  $\omega = 0.2$ . The action is derived such that rotational invariance of the free fermion propagator is restored up to  $O(p^4)$ . It is known that this action makes the discretization error of the equation of state pressure  $p(T)$  small as  $T \rightarrow \infty$ , and  $T_c$  obtained by this action is consistent with that obtained using improved Wilson fermions [13,15]. To incorporate the chemical potential, we generalise the standard prescription of treating  $\mu$  as an imaginary gauge potential  $A_0$  [16] by multiplying the terms generating  $n$ -step hops in the positive and negative temporal directions by  $e^{n\mu}$  and  $e^{-n\mu}$  respectively<sup>3</sup>.

We investigated the transition points for quark masses  $m = 0.1$  and  $0.2$ . The corresponding pseudoscalar and vector meson mass ratios are  $m_P/m_V \approx 0.70$  and  $0.85$  [13]. We compute the Polyakov loop, chiral condensate, and their susceptibilities. The simulations were performed on a  $16^3 \times 4$  lattice for 7 values of  $\beta \in [3.64, 3.67]$  for  $m = 0.1$  and 6 values of  $\beta \in [3.74, 3.80]$  for  $m = 0.2$ , using the Hybrid R algorithm. We adopted a step size  $\Delta\tau = 0.25 \times m$  and a molecular dynamics trajectory length  $\tau = 0.5$ . For each trajectory 10 sets of  $Z_2$  noise vectors were used to calculate the reweighting factor and the derivatives of  $\bar{\psi}\psi$  up to second order in  $\mu$ .

For the calculation of mass reweighting surveyed in Sec. IV, we took a total of 220600 trajectories at  $m = 0.1$  and 155000 trajectories at  $m = 0.2$ . For the study with  $\mu \neq 0$  described in Sec. V, we used 128000 trajectories at  $m = 0.1$  and 86000 trajectories at  $m = 0.2$ . The details are summarized in Table I. The multi-histogram method of [11] was used to reweight in the  $\beta$ -direction using data from several values of  $\beta$ . Errors were estimated using the jack-knife method with bin size 100 trajectories.

#### IV. REWEIGHTING FOR QUARK MASS

Before calculating derivatives with respect to  $\mu$ , it is worthwhile to calculate the derivatives with respect to quark mass  $m$ , which is not only potentially important for the chiral extrapolation, but also a good demonstration of the reweighting technique for a parameter appearing in the fermion action. Because we cannot compare the result obtained by reweighting in the  $\mu$  direction with the result of an actual simulation at  $\mu \neq 0$ , this test is a necessary check of

<sup>3</sup> Note that for any improved action involving terms in which  $\psi$  and  $\bar{\psi}$  are separated by more than a single link, there is no longer a local conserved baryon number current  $j_\mu(x)$  such that  $\sum_\mu \langle j_\mu(x) - j_\mu(x-\hat{\mu}) \rangle = 0$  for non-zero lattice spacing.

the reliability of our method. The reweighting formula for quark mass is easily obtained from eqn. (4) and eqns. (7) by replacing  $\partial^n M / \partial \mu^n$  with  $\partial M / \partial m = 1$  and  $\partial^n M / \partial m^n = 0$  for  $n \geq 2$ . In the case of the reweighting for  $m$ , we compute the fermionic reweighting factor up to second order, and the chiral condensate up to first order, i.e.

$$\ln \det M(m) - \ln \det M(m_0) = \text{tr} M^{-1}(m - m_0) - \text{tr}(M^{-1}M^{-1})(m - m_0)^2/2 + O[(m - m_0)^3], \quad (22)$$

$$\bar{\psi}\psi = (N_s^3 N_t)^{-1} \alpha N_f [\text{tr} M^{-1} - \text{tr}(M^{-1}M^{-1})(m - m_0)] + O[(m - m_0)^2]. \quad (23)$$

Hence, the error of the Polyakov loop susceptibility is  $O[(m - m_0)^3]$  and that of the chiral susceptibility  $O[(m - m_0)^2]$ . Figures 1 and 2 show  $\chi_L$  and Figs. 3 and 4 show  $\chi_{\bar{\psi}\psi}$  for different  $m$  as functions of  $\beta$  for simulation masses  $m_0 = 0.1$  and  $0.2$ . These figures show that the peak position moves to smaller  $\beta$  as  $m$  decreases as expected. Moreover we find that as  $m$  decreases the peak height becomes lower for  $\chi_L$  and higher for  $\chi_{\bar{\psi}\psi}$ . These behaviours are consistent since the Polyakov loop is an exact order parameter only in the limit  $m \rightarrow \infty$ , while the chiral condensate is an order parameter only for  $m \rightarrow 0$ . The phase transition is known to be a crossover for 2 flavor QCD with  $m > 0$ . We calculate the slope of the transition point  $\partial \beta_c / \partial m$  assuming that  $\beta_c(m)$  is defined by the peak position of the susceptibility whenever a clear peak is obtained<sup>4</sup>. Figures 5, 6 and 7 show  $\beta_c(m)$  for each  $m_0$ . We fit the data by a power series expansion about  $m_0$ , i.e.,  $\beta_c(m) = \beta_c(m_0) + \sum_{n=1}^{N_{\text{fit}}} c_n (m - m_0)^n$ , with fit range  $|(m - m_0)/m_0| \leq 0.05$  or  $0.1$ . The results are presented in Table II. We find a linear fit to be adequate with the dependence on choice of  $N_{\text{fit}}$  less than 3%; the discrepancy from the choice of fit range is less than 10%. Both uncertainties lie well within the statistical error. We denote the fitted line for  $N_{\text{fit}} = 1$  and  $|(m - m_0)/m_0| \leq 0.1$  by a dashed line. In Fig. 8 we compare the predicted variation of  $\beta_c(m)$  with previously existing data [13]. Filled symbols are the results of the current study. The short lines denote the upper and lower bounds on the slope  $\beta'_c$ . From this figure, we find that reweighting yields results which are quite consistent with those of direct simulation, and hence infer that reweighting the fermion action using the technique we have outlined works well.

## V. REWEIGHTING FOR CHEMICAL POTENTIAL

### A. Chemical potential dependence of the transition temperature

Next we turn our attention to reweighting with respect to  $\mu$ , with the Taylor expansion made about the simulation point  $\mu = 0$ . First we calculate the derivatives of the transition point with respect to  $\mu$  in the region of small  $\mu$  relevant to RHIC. In Figs. 9, 10, 11 and 12, we plot  $\chi_L$  and  $\chi_{\bar{\psi}\psi}$  at  $m = 0.1$  and  $0.2$  for various  $\mu$ . As outlined in section II, we compute consistently up to  $O(\mu^2)$  and expect the results to contain errors at  $O(\mu^4)$ . Strictly speaking, the  $O(\mu^3)$  term does not vanish for  $L$  since it is complex (see Sec. II). However, we expect that  $\chi_L$  and  $\chi_{\bar{\psi}\psi}$  yield the same  $\beta_c$  (see below) with error  $O(\mu^4)$ . The figures show that the position of the susceptibility peak moves lower as  $\mu$  increases, which means that the critical temperature becomes lower as  $\mu$  increases. As we obtained well-localised peaks for  $\chi_L$  at  $m = 0.2$  and  $\chi_{\bar{\psi}\psi}$  at  $m = 0.1$  and  $0.2$ , we use these peak positions to determine the transition point  $\beta_c$  as functions of  $\mu^2$  in Figs. 13, 14, and 15. Note that because the Polyakov loop is interpreted as an external quark current running in the positive time direction, positive and negative  $\mu$  give different contributions to both  $L$  and  $\chi_L$ , and we display both cases. Figs. 13, 14 and 15 also display the value of  $\mu = 0.1 T_c$  relevant for RHIC. The shift  $\beta_c(\mu) - \beta_c(0)$  is found to be small at this point.

Because the first derivative is expected to be zero as discussed above, we fit the  $\beta_c$  data by a straight line in  $\mu^2$ , fixing  $\beta_c$  at  $\mu = 0$ , in ranges  $\mu^2 \leq 0.008(0.014)$  for  $m = 0.1(0.2)$  respectively, in which the phase problem is not serious (see Sec. V C below). We obtain  $d^2 \beta_c / d\mu^2 = -1.20(44)$  and  $-1.02(56)$  at  $m = 0.1$  and  $0.2$  from the chiral susceptibility and  $d^2 \beta_c / d\mu^2 = -1.01(23)$  at  $m = 0.2$  from the Polyakov loop susceptibility. Dot-dashed lines in Figs. 13, 14 and 15 are the fitted lines. To investigate the fit range dependence and the fitting function dependence, we also tried the range  $\mu^2 \leq 0.005(0.01)$  for  $m = 0.1(0.2)$ , and using a quadratic fit function. Table III summarises the results. We may conclude that  $|d^2 \beta_c / d\mu^2| \approx 1.1$  with 30–50% error, and any quark mass dependence of  $d^2 \beta_c / d\mu^2$  is not visible within the accuracy of our calculation.

Of course, it is desirable to translate these observations into physical units. The second derivative of  $T_c$  can be estimated by

---

<sup>4</sup> Because the peak width of  $\chi_L$  is too wide for the smaller mass  $m = 0.1$ , we do not determine the pseudocritical point for  $L$  in this case.

$$\frac{d^2 T_c}{d\mu_q^2} = -\frac{1}{N_t^2 T_c} \frac{d^2 \beta_c}{d\mu^2} \left/ \left( a \frac{d\beta}{da} \right) \right., \quad (24)$$

where  $a$  is the lattice spacing. The beta-function may be obtained from the string tension data in Ref. [13]. We compute it by differentiating the interpolation function of the string tension with an ansatz [17]:

$$\sqrt{\sigma a^2}(\beta) = R(\beta)(1 + c_2 \hat{a}^2(\beta) + c_4 \hat{a}^4(\beta))/c_0, \quad (25)$$

where  $R(\beta)$  is the usual 2-loop scaling function,  $\hat{a} \equiv R(\beta)/R(\bar{\beta})$  and  $\bar{\beta} = 3.70$ .  $c_0, c_2$  and  $c_4$  are fit parameters with  $c_0 = 0.0570(35), c_2 = 0.669(208)$  and  $c_4 = -0.0822(1088)$  at  $m = 0.1$ . We get  $a^{-1}(da/d\beta) = -2.08(43)$  at  $(\beta, m) = (3.65, 0.1)$ . We then find  $T_c(d^2 T_c/d\mu_q^2) \approx -0.14$  at  $m = 0.1$ . We sketch the phase transition line with 50% error in Fig. 16 assuming  $T_c \simeq 170$  MeV. On the assumption that the transition line is parabolic all the way down to  $T = 0$ , then this curvature is too small to be consistent with the phenomenological expectation that at  $T = 0$  a transition from hadronic to quark matter occurs for  $\mu_c$  some 50 - 200 MeV greater than the onset of nuclear matter at  $\mu_o \simeq m_N/3 \simeq 307$  MeV [18]. This tendency is also supported by the result of Fodor and Katz [7], and hints at contributions from higher-order derivatives, or even non-analytic behaviour, at larger values of  $\mu$ . Despite the large errors we can see that our result gives us useful information about the phase diagram, at least for small  $\mu$ , because the first derivative is zero.

Another point worth noting is the screening effect of dynamical anti-quarks at  $\mu < 0$ . Negative chemical potential induces the dynamical generation of anti-quarks, which in contrast to quarks can completely screen an external color triplet current. Thus the free energy of a single quark is reduced, especially in the confinement phase, and the singularity at the phase transition point is weakened due to the reduction in the range of current-current interactions. This effect can be seen in Figs. 9, 10, 17 and 18, where we denote the Polyakov loop and its susceptibility at  $\mu < 0$  by dot-dot-dash and dot-dash-dash lines. We see that  $L$  at  $\mu < 0$  is larger than that at  $\mu > 0$ , which means that the free energy at  $\mu < 0$  is smaller. Moreover, as seen in Fig. 10, the peak height of  $\chi_L$  becomes smaller for  $\mu < 0$ , while the position of the pseudocritical line in Fig. 13 is almost the same between positive and negative  $\mu$ . The screening effect only seems to make the phase transition singularity weaker without shifting the pseudocritical line. Because the only source of asymmetry between  $\mu$  and  $-\mu$  is due to the correlation between the imaginary parts of the fermion determinant and  $L$ , these imaginary contributions help to decrease the susceptibility at  $\mu < 0$ . In this way, we can see that the explicit breaking of time reversal symmetry by exchange of  $\mu$  with  $-\mu$  helps to highlight an interesting feature of dynamical quarks in full QCD.

Finally, if instead we were to impose an isovector chemical potential  $\mu_I$  having opposite sign for  $u$  and  $d$  quarks [9,19], then the quark determinant would become real and positive, enabling simulations using standard Monte-Carlo methods [20]. This motivates a comparison between systems with the usual isoscalar chemical potential  $\mu$  and the isovector chemical potential  $\mu_I$ . In the framework of the Taylor expansion, terms even in  $\mu$  are identical for both  $u$  and  $d$  quarks, but odd terms cancel for the case  $\mu_I \neq 0$ , meaning that terms proportional to  $\mathcal{O}_1, \mathcal{R}_1$  should be set to zero in eqn. (14). We analyzed the transition point  $\beta_c(\mu_I)$  for  $m = 0.2$ ; the results are shown in Fig. 19 for  $\beta_c$  determined by  $\chi_L$  and Fig. 20 for that by  $\chi_{\bar{\psi}\psi}$ . The solid line shows  $\beta_c$  as a function of  $\mu_I$ , the dashed line  $\beta_c(\mu)$ . The second derivative of  $\beta_c$  with respect to  $\mu_I$  is found to be  $-0.96(19)$  for  $\chi_L$  and  $-0.93(52)$  for  $\chi_{\bar{\psi}\psi}$ . Dot-dashed lines in Figs 19 and 20 show the fits. Within errors there appears to be no significant difference between isovector and isoscalar chemical potentials for small  $\mu$ . A similar analysis for  $\chi_{\bar{\psi}\psi}$  at  $m = 0.1$  is shown in Fig. 21; here the second derivative of  $\beta_c$  is  $-0.71(16)$ , which is smaller than the isoscalar case. However this result is also smaller than that obtained at  $m = 0.2$ , which is physically unacceptable since the second derivative should approach zero as  $m \rightarrow \infty$ . Hence the difference between  $\mu_I$  and  $\mu$  at  $m = 0.1$  is most likely due to statistical error.

The terms we have dropped are associated with fluctuations in the phase of  $\det M$ , which are small in the region of small  $\mu$ , as will be demonstrated in Sec. V C below. This is perhaps not unexpected on physical grounds – increasing  $\mu_I$  is predicted to induce the onset of matter in the form of a pion condensate at a critical  $\mu_{Io} \simeq m_{PS}/2$  [19], and indeed evidence for this scenario in the form of a negative curvature for  $m_{PS}(\mu_I)$  in the low  $T$  phase is reported in [10]. However, even for  $m = 0.1$  on this lattice this scale is roughly  $0.92\sqrt{\sigma} \simeq 390$  MeV [13], which is a little larger than the isoscalar onset threshold  $\mu_o \lesssim m_N/3$ . The curvature with respect to  $\mu_I$  should dominate as the chiral limit is approached and pion and nucleon mass scales become separate. If this turns out to be the case, then it is interesting to note that phase correlations between observable and measure actually *decrease* the physical effect of raising  $\mu$ ; this has also been observed in simulations of two-color QCD with a single flavor of staggered adjoint quark [21], in which including the sign of the fermion determinant has the effect of postponing the onset transition.

## B. Quark number susceptibility and equation of state at $\mu \neq 0$

The energy density  $\epsilon$  and pressure  $p$  at the critical point are interesting quantities for heavy-ion collision experiments. In this section, we discuss the  $\mu$ -dependence of the equation of state which describes them. If we employ the integral method based on the homogeneity of the system [22], we obtain  $p = (T/V) \ln \mathcal{Z}$ ; derivatives of  $p$  with respect to  $\mu$  are then related to the quark number density  $n_q$  (via a Maxwell relation) and the singlet quark number susceptibility  $\chi_S = \partial n_q / \partial \mu_q$  [8]:

$$\frac{\partial(p/T^4)}{\partial \mu_q} = \frac{1}{VT^3} \frac{\partial \ln \mathcal{Z}}{\partial \mu_q} = \frac{n_q}{T^4} \quad (26)$$

$$\frac{\partial^2(p/T^4)}{\partial \mu_q^2} = \frac{1}{VT^3} \frac{\partial^2 \ln \mathcal{Z}}{\partial \mu_q^2} = \frac{\chi_S}{T^4} \quad (27)$$

Here  $n_q$ ,  $\chi_S$  and also the nonsinglet susceptibility  $\chi_{NS}$  are given in physical units by

$$\frac{n_q}{T^3} = \frac{\alpha N_f N_t^2}{N_s^3} \left\langle \text{tr} \left( M^{-1} \frac{\partial M}{\partial \mu} \right) \right\rangle. \quad (28)$$

$$\begin{aligned} \frac{\chi_S}{T^2} &= \frac{\alpha N_f N_t}{N_s^3} \left[ \left\langle \text{tr} \left( M^{-1} \frac{\partial^2 M}{\partial \mu^2} \right) \right\rangle - \left\langle \text{tr} \left( M^{-1} \frac{\partial M}{\partial \mu} M^{-1} \frac{\partial M}{\partial \mu} \right) \right\rangle \right] \\ &\quad + \frac{(\alpha N_f)^2 N_t}{N_s^3} \left[ \left\langle \text{tr} \left( M^{-1} \frac{\partial M}{\partial \mu} \right) \text{tr} \left( M^{-1} \frac{\partial M}{\partial \mu} \right) \right\rangle - \left\langle \text{tr} \left( M^{-1} \frac{\partial M}{\partial \mu} \right) \right\rangle^2 \right], \end{aligned} \quad (29)$$

$$\frac{\chi_{NS}}{T^2} = \frac{\alpha N_f N_t}{N_s^3} \left[ \left\langle \text{tr} \left( M^{-1} \frac{\partial^2 M}{\partial \mu^2} \right) \right\rangle - \left\langle \text{tr} \left( M^{-1} \frac{\partial M}{\partial \mu} M^{-1} \frac{\partial M}{\partial \mu} \right) \right\rangle \right], \quad (30)$$

The quark number density is zero at  $\mu = 0$  so once again the leading correction is  $O(\mu^2)$ . The susceptibilities  $\chi_{SA}a^2$ , and  $\chi_{NS}a^2$  are plotted in Figs. 22 and 23 for  $m = 0.1$  and  $0.2$ . Because  $\chi_{SA}a^2 \approx 0.043(0.030)$  at  $\beta_c$  for  $m = 0.1(0.2)$ , we obtain  $T^2 \partial^2(p/T^4)/\partial \mu_q^2 \approx 0.69$  ( $m = 0.1$ ) and  $0.48$  ( $m = 0.2$ ). The discrepancy of  $p/T^4$  at the interesting point for RHIC,  $\mu_q/T_c \sim 0.1$ , from its value at  $\mu = 0$  is about  $0.0034(0.0024)$  for  $m = 0.1(0.2)$ ; since  $p/T^4 \approx 0.27$  at  $\beta_c$  for  $(m, \mu) = (0.1, 0)$  [13] this is a 1% effect, and hence quite small. We can also obtain estimates of the quark number density via  $n_q a^3 \simeq \mu_q a \chi_{SA} a^2$ , with results  $n_q/T^3 = 0.688(0.480) \mu_q/T$  for  $m = 0.1(0.2)$  which assuming  $T \simeq 170$  MeV translates into roughly 10%(6%) of nuclear matter density at the RHIC point. Clearly these values will need careful extrapolation to the chiral limit before a meaningful comparison with experiment can be made.

Moreover the energy density  $\epsilon$  can also be estimated via the equation for the conformal anomaly:

$$\begin{aligned} \frac{\epsilon - 3p}{T^4} &= -\frac{1}{VT^3} a \frac{\partial \ln \mathcal{Z}}{\partial a} \\ &= -\frac{1}{VT^3} \left[ a \frac{\partial \beta}{\partial a} \frac{\partial \ln \mathcal{Z}}{\partial \beta} + a \frac{\partial m}{\partial a} \frac{\partial \ln \mathcal{Z}}{\partial m} \right]. \end{aligned} \quad (31)$$

Here we estimate  $\epsilon$  in the chiral limit, where  $a \partial m / \partial a$  can be neglected. We find

$$\frac{\epsilon - 3p}{T^4} \approx -\frac{1}{VT^3} \frac{\partial \ln \mathcal{Z}}{\partial \beta} \left( \frac{1}{a} \frac{\partial a}{\partial \beta} \right)^{-1}, \quad (32)$$

with second derivative

$$\frac{\partial^2((\epsilon - 3p)/T^4)}{\partial \mu_q^2} \approx -\frac{1}{T^4} \frac{\partial \chi_S}{\partial \beta} \left( \frac{1}{a} \frac{\partial a}{\partial \beta} \right)^{-1}. \quad (33)$$

Because the quark mass dependence of the equation of state seems to be small in Ref. [23], we estimate the derivative using the value of  $\chi_S$  at  $m = 0.1$  and  $0.2$ . From Figs. 22 and 23, we obtain  $\partial(\chi_{SA}a^2)/\partial \beta \approx 1.05(0.81)$  at  $\beta_c$  for  $m = 0.1(0.2)$ . Then the second derivative of  $\epsilon - 3p$  is estimated to be  $\partial^2((\epsilon - 3p)/T^4)/\partial \mu_q^2 \approx 8.1/T^2$  at  $m = 0.1$ , where we use the same value of the beta-function as in Sec. V A. Finally, we obtain  $\partial^2(\epsilon/T^4)/\partial \mu_q^2 \approx 10/T^2$ . The discrepancy of  $\epsilon/T^4$  at the RHIC point from  $\mu = 0$  is about 0.05. Once again, because  $\epsilon/T^4 \approx 6$  at  $\beta_c$  for  $(m, \mu) = (0.1, 0)$  [24], this is a 1% effect, suggesting that the  $\mu_q$ -dependence of the equation of state is small in the regime of relevance for RHIC.

Next we discuss the relation between the equation of state and the phase transition line. It is of great interest to investigate whether the values of the pressure  $p(T_c(\mu_q), \mu_q)$  and energy density  $\epsilon(T_c(\mu_q), \mu_q)$  along the transition line are constant or not. To this end, consider the line of constant pressure in the  $(T, \mu_q)$  plane, i.e.,

$$\Delta p = \frac{\partial p}{\partial T} \Delta T + \frac{\partial p}{\partial (\mu_q^2)} \Delta (\mu_q^2) = \left[ T^4 \frac{\partial (p/T^4)}{\partial T} + \frac{4p}{T} \right] \Delta T + \left[ T^4 \frac{\partial (p/T^4)}{\partial (\mu_q^2)} \right] \Delta (\mu_q^2) = 0, \quad (34)$$

together with a similar relation for  $\Delta \epsilon$ , and compare it with the phase transition line. The slope of the constant pressure line is then given by

$$\frac{dT}{d(\mu_q^2)} = - \frac{\partial (p/T^4)}{\partial (\mu_q^2)} / \left( \frac{\partial (p/T^4)}{\partial T} + \frac{4p}{T^5} \right). \quad (35)$$

The derivative  $\partial(p/T^4)/\partial T$  can be calculated by

$$T \frac{\partial (p/T^4)}{\partial T} = - \left( \frac{1}{a} \frac{\partial a}{\partial \beta} \right)^{-1} \frac{\partial (p/T^4)}{\partial \beta} = \left( \frac{1}{a} \frac{\partial a}{\partial \beta} \right)^{-1} N_t^4 \left( \left\langle \frac{S_g}{N_s^3 N_t} \right\rangle - \left\langle \frac{S_g}{N_s^3 N_t} \right\rangle_0 \right), \quad (36)$$

where  $\langle \cdots \rangle_0$  means the expectation value evaluated at  $T = 0$  for normalization. Using the data of Ref. [13],  $p/T^4 = 0.27(5)$ ,  $\partial(p/T^4)/\partial \beta = 4.5(9)$  at  $T_c$  for  $m = 0.1$ , together with the beta-function in Sec. V A, we obtain  $T(\partial(p/T^4)/\partial T)|_{T=T_c} = 2.2(6)$  for  $m = 0.1$ . Noting also that  $\partial(p/T^4)/\partial (\mu_q^2) = (1/2)(\partial^2(p/T^4)/\partial \mu_q^2) = 0.344(4)/T^2$ , we find that the slope of the constant pressure line emerging from the critical point on the  $T$ -axis is  $T(dT/d(\mu_q^2)) = -0.106(21)$ . A similar argument using the data of [24] gives the slope of the constant energy density line  $T(dT/d(\mu_q^2)) = -0.081(20)$ . Because the slope of the transition line in terms of  $\mu_q^2$  is  $T_c(dT_c/d(\mu_q^2)) = (1/2)T_c(d^2T_c/d\mu_q^2) \approx -0.07(3)$ , we deduce that the variations of  $p$  and  $\epsilon$  along the phase transition line are given by

$$p(T_c(\mu_q), \mu_q) - p(T_c(0), 0) = \mu_q^2 T_c^2(0) \times 0.12(11) ; \quad \epsilon(T_c(\mu_q), \mu_q) - \epsilon(T_c(0), 0) = \mu_q^2 T_c^2(0) \times 0.7(2.2), \quad (37)$$

the dominant source of uncertainty in each case being the location of the phase transition line itself. Within our errors, therefore, both pressure and energy density appear constant along the phase transition line.

### C. The phase of the determinant at $\mu \neq 0$

Finally we discuss the region of applicability of generic reweighting approaches. If the reweighting factor in eqn. (1) changes sign frequently due to the complex phase of the quark determinant, then both numerator and denominator of (1) become vanishingly small in the thermodynamic limit, typically behaving  $\sim e^{-N_{\text{site}}}$  with the lattice size  $N_{\text{site}} \equiv N_s^3 N_t$ . This makes control of statistical errors in the calculation of the expectation value very difficult. Of course,  $\arg(\det M)$  starts at zero at  $\mu = 0$  but grows as  $\mu$  increases. It is important to establish at which value of  $\mu$  the sign problem becomes severe.

As discussed in section II, the phase can be expressed using the odd terms of the Taylor expansion of  $\ln \det M$ . If we write  $\det M = |\det M| e^{i\theta}$ , then

$$\theta = \alpha N_f \text{Im} \left[ \mu \frac{\partial \ln \det M}{\partial \mu} + \frac{\mu^3}{3!} \frac{\partial^3 \ln \det M}{\partial \mu^3} + \dots \right]. \quad (38)$$

For small  $\mu$ , the first term  $\alpha N_f \text{Im} \text{tr}[M^{-1}(\partial M \partial \mu)] \mu$  is dominant. Now, because  $(N_s^3 N_t)^{-1} \text{tr}[M^{-1}(\partial M \partial \mu)]$  is the quark number density, its expectation value must be real and in fact vanishes at  $\mu = 0$ . Although the average of the phase is zero, its fluctuations remain important. We investigated the standard deviation of  $(N_s^3 N_t)^{-1} \text{Im} \text{tr}[M^{-1}(\partial M \partial \mu)]$  and present the results in Table IV. We find values of about  $2.2 \times 10^{-3}$  at  $\beta_c(m = 0.1)$  and  $1.6 \times 10^{-3}$  at  $\beta_c(m = 0.2)$ . The standard deviation of the leading term of (38) therefore has a magnitude of about  $18\mu$  for  $m = 0.1$  and  $13\mu$  for  $m = 0.2$  in the vicinity of the transition. Consequently the phase problem appears from  $\mu \sim 0.09(0.12)$ , i.e.,  $\mu_q/T_c \sim 0.4(0.5)$  for  $m = 0.1(0.2)$ , since the phase problem arises if the phase fluctuation becomes of  $O(1)$ . We notice that the value of  $\mu$  for which the phase fluctuations become significant decreases as either  $m$  or  $\beta$  decreases. Roughly speaking, the numerator and denominator of (2) decrease in proportion to the average of the phase factor  $\langle \text{Re}(e^{i\theta}) \rangle$ . We show this factor for various  $\beta$  and  $m$  in Fig. 24, where it is clear that the average becomes small around the values of  $\mu$  quoted above. The phase fluctuations at the RHIC point  $\mu_q = 0.17_c$ , however, are small enough for the analysis of secs. V A and V B to be applicable.

We should also note that the fluctuation of the phase depends on the lattice size  $N_{\text{site}}$ , and on the number of the noise vectors  $N_n$ . From general arguments, the phase of the reweighting factor is expected to decrease as  $\langle e^{i\theta} \rangle \propto e^{-N_{\text{site}}}$ , implying that the applicable region of reweighting becomes narrower as the lattice size grows. By contrast, the value of  $\text{Im} \text{tr}[M^{-1}(\partial M / \partial \mu)]$  calculated on each configuration also contains an error due to the finite number of noise vectors (see eqn.(40) of the Appendix); for  $N_n = 10$  this error is not small compared to the standard deviation, as seen in Table IV. The phase fluctuation discussed above includes this error due to finite  $N_n$ , and we suspect that the true fluctuation becomes smaller as  $N_n$  increases. To confirm this, we reanalyze the standard deviation  $\sqrt{\langle \{\text{Im} \text{tr}[M^{-1}(\partial M / \partial \mu)]\}^2 \rangle - \langle \text{Im} \text{tr}[M^{-1}(\partial M / \partial \mu)] \rangle^2}$  by treating the calculation of  $\langle \{\text{Im} \text{tr}[M^{-1}(\partial M / \partial \mu)]\}^2 \rangle$  more carefully. Since the noise sets must be independent, we subtract the contributions from using the same noise vector for each factor. Details are given in the Appendix. The results are quoted in the STD(Imp.) column of Table IV and are found to be significantly smaller. Because they might be closer to the  $N_n = \infty$  limit, they suggest that the standard deviation for larger  $N_n$  is much smaller, which means that the region of applicability becomes wider as  $N_n$  increases.

## VI. CONCLUSIONS

In this paper we have proposed a new method based on a Taylor expansion in chemical potential  $\mu$  to investigate the thermodynamic properties of QCD with  $\mu \neq 0$ . By computing the chiral susceptibility and the Polyakov loop susceptibility for 2 flavors of p-4 improved staggered fermions, we have been able to estimate the dependence of  $\beta_c$ , and hence the critical temperature  $T_c$ , on  $\mu$  on moderately large volumes, thus reinforcing the recent advance of lattice QCD into the interior of the  $(\mu_q, T)$  plane [4]. We have also been able to quantify the effect of a non-zero chemical potential on the equation of state. Although we have focussed on critical observables in order to fix physical scales, the method can be applied in a small range of  $\mu$  at arbitrary  $\beta$ , although the radius of convergence is expected to decrease as  $T \rightarrow 0$  since in this limit all  $\mu$ -dependence should vanish for  $\mu_q \leq \mu_o$ , making the behaviour about the origin non-analytic. The method is also applicable to a range of physical observables [8–10]. We find that  $T_c$  decreases as  $\mu$  increases, but this appears to depend only weakly on quark mass, an effect also observed in studies of the equation of state  $p(T)$  [23]. Our results are in broad agreement with estimates based on exact reweighting [7] and suggest that the discrepancy of  $\beta_c$  from its value at  $\mu = 0$  is small in the interesting region for heavy-ion collisions. Moreover we have observed evidence that when a negative chemical potential is imposed, the generation of dynamical anti-quarks and the consequent screening of an external color triplet current is enhanced.

An unresolved issue is the method's limitations. We have been able to estimate the complex phase of the fermion determinant for a  $16^3 \times 4$  lattice and found that the sign problem is not serious in the range  $\mu_q/T_c < 0.4\text{--}0.5$  for  $m = 0.1\text{--}0.2$ , covered by this study. It is not yet clear to us to what extent the radius of convergence of the Taylor expansion is linked to the fluctuations of  $\text{arg}(\det M)$ . An optimist might hope that the method can yield accurate thermodynamic information all the way out to the critical endpoint where the quark/hadron phase transition changes from second to first order; moreover, since individual terms in the expansion are expectation values of local operators, the method should be applicable on arbitrarily large volumes, particularly if larger numbers  $N_n$  of stochastic noise vectors than we have used here are employed. A pessimist might worry that phase fluctuations should make calculation of higher order terms impracticable long before the radius of convergence is reached, particularly as the chiral limit is approached since in this case the correlations between  $\text{arg}(\det M)$  and  $\text{Im}(\mathcal{O})$  should discriminate between the different physics associated with isoscalar and isovector chemical potentials. More work is needed before we can say which is more realistic.

## ACKNOWLEDGMENTS

Numerical work was performed using a 128-processor APEmille in Swansea. This work was supported by PPARC grant PPA/G/S/1999/00026, by the EU contract ERBFMRX-CT97-0122, and by the National Science Foundation under Grant No. PHY99-07949.

---

[1] U. Heinz, Nucl. Phys. A685 (2001) 414.

- [2] K. Rajagopal and F. Wilczek, in *At the Frontier of Particle Physics: Handbook of QCD* ed. M. Shifman, p. 2061 (World Scientific, Singapore) (2001).
- [3] S. Ejiri, Nucl. Phys. Proc. Suppl. 94 (2001) 19.
- [4] S.J. Hands, Nucl. Phys. Proc. Suppl. 106 (2002) 142.
- [5] P. Braun-Munzinger, D. Magestro, K. Redlich and J. Stachel, Phys. Lett. B518 (2001) 41.
- [6] I.M. Barbour and A.J. Bell, Nucl. Phys. B372 (1992) 385;  
I.M. Barbour, S.E. Morrison, E.G. Klepfish, J.B. Kogut and M.-P. Lombardo, Phys. Rev. D56 (1997) 7063.
- [7] Z. Fodor and S.D. Katz, hep-lat/0104001; hep-lat/0106002.
- [8] S. Gottlieb *et al.*, Phys. Rev. D38 (1988) 2888.
- [9] R.V. Gavai and S. Gupta, Phys. Rev. D64 (2001) 074506; hep-lat/0202006;  
R.V. Gavai, S. Gupta and P. Majumdar, hep-lat/0110032.
- [10] QCDSF Collaboration, S. Choe *et al.*, Phys. Rev. D65 (2002) 054501.
- [11] A.M. Ferrenberg and R.H. Swendsen, Phys. Rev. Lett. 61 (1988) 2635; Phys. Rev. Lett. 63 (1989) 1195.
- [12] U.M. Heller, F. Karsch, and B. Sturm, Phys. Rev. D60 (1999) 114502.
- [13] F. Karsch, E. Laermann, and A. Peikert, Phys. Lett. B478 (2000) 447; Nucl. Phys. B605 (2001) 579.
- [14] F. Karsch, E. Laermann, and Ch. Schmidt, Phys. Lett. B520 (2001) 41.
- [15] CP-PACS Collaboration, A. Ali Khan *et al.*, Phys. Rev. D63 (2000) 034502.
- [16] P. Hasenfratz and F. Karsch, Phys. Lett. 125B (1983) 308;  
J.B. Kogut *et al.*, Nucl. Phys. B225 (1983) 93.
- [17] C.R. Allton, hep-lat/9610016.
- [18] S.P. Klevansky, Rev. Mod. Phys. 64 (1992) 649;  
M.A. Halasz, A.D. Jackson, R.E. Shrock, M.A. Stephanov and J.J.M. Verbaarschot, Phys. Rev. D58 (1998) 096007.
- [19] D.T. Son and M.A. Stephanov, Phys. Rev. Lett. 86 (2001) 592.
- [20] J.B. Kogut and D.K. Sinclair, hep-lat/0201017, hep-lat/0202028;  
S. Gupta, hep-lat/0202005.
- [21] S.J. Hands, I. Montvay, S.E. Morrison, M. Oevers, L. Scorzato and J. Skullerud, Eur. Phys. J. C17 (2000) 285;  
S.J. Hands, I. Montvay, L. Scorzato and J. Skullerud, Eur. Phys. J. C22 (2001) 451.
- [22] J. Engels, J. Fingberg, F. Karsch, D. Miller and M. Weber, Phys. Lett. B252 (1990) 625.
- [23] CP-PACS Collaboration, A. Ali Khan *et al.*, Phys. Rev. D64 (2001) 074510.
- [24] F. Karsch, Nucl. Phys. A698 (2002) 199.

## APPENDIX: REMARK ON THE NOISE METHOD

The calculation of an operator such as  $(\text{tr}A)^2$ , where  $A$  is a matrix, using the noise method has to be treated carefully. Because the random noise vectors should be independent for each calculation of  $\text{tr}A$ ,

$$(\text{tr}A)^2 = \lim_{N_n \rightarrow \infty} \frac{1}{N_n} \sum_{a=1}^{N_n} \eta_a^\dagger A \eta_a \frac{1}{N_n} \sum_{b=1}^{N_n} \eta_b^\dagger A \eta_b = \lim_{N_n \rightarrow \infty} \frac{1}{N_n(N_n - 1)} \sum_{a \neq b} \eta_a^\dagger A \eta_a \eta_b^\dagger A \eta_b. \quad (39)$$

This equation can be rewritten as

$$(\text{tr}A)^2 = \lim_{N_n \rightarrow \infty} \left[ \left( \frac{1}{N_n} \sum_a \eta_a^\dagger A \eta_a \right)^2 - \varepsilon^2(A) \right], \quad (40)$$

where  $\varepsilon(A)$  is the error due to finite  $N_n$ :

$$\varepsilon^2(A) = \frac{1}{N_n - 1} \left\{ \frac{1}{N_n} \sum_a \left( \eta_a^\dagger A \eta_a \right)^2 - \left( \frac{1}{N_n} \sum_a \eta_a^\dagger A \eta_a \right)^2 \right\}. \quad (41)$$

The error decreases as  $(N_n - 1)^{-1}$  as  $N_n$  increases, but can be significant for small  $N_n$ . Moreover,  $\varepsilon^2(A)$  is negligible for an operator which always has the same sign such as  $\text{tr}M^{-1}$ ; in this case its contribution is about 0.001% for  $\langle (\text{tr}M^{-1})^2 \rangle$  with  $N_n = 10$ . However, for an operator which changes sign frequently such as  $\text{tr}[M^{-1}(\partial M / \partial \mu)]$ , the effect of the additional term is important. We calculate the quark number susceptibility and the value of ‘STD(Imp.)’ in Table IV taking this additional term into account. The difference between ‘STD’ and ‘STD(Imp.)’ in Table IV is the contribution from the additional term.

Next, we construct the reweighting method based on Taylor expansion, eqn.(2), explicitly up to second order using the noise method. Assuming  $\mathcal{O}$  is a bosonic operator, we can rewrite the numerator of eqn.(2):

$$\begin{aligned} \left\langle \mathcal{O} e^{\alpha N_f (\ln \det M(m, \mu) - \ln \det M(m_0, 0))} \right\rangle &= \langle \mathcal{O} \rangle + \mu \alpha N_f \left\langle \mathcal{O} \text{tr} \left( M^{-1} \frac{\partial M}{\partial \mu} \right) \right\rangle \\ &+ \frac{\mu^2}{2} (\alpha N_f)^2 \left\langle \mathcal{O} \text{tr} \left( M^{-1} \frac{\partial M}{\partial \mu} \right) \text{tr} \left( M^{-1} \frac{\partial M}{\partial \mu} \right) \right\rangle \\ &+ \frac{\mu^2}{2} \alpha N_f \left[ \left\langle \mathcal{O} \text{tr} \left( M^{-1} \frac{\partial^2 M}{\partial \mu^2} \right) \right\rangle - \left\langle \mathcal{O} \text{tr} \left( M^{-1} \frac{\partial M}{\partial \mu} M^{-1} \frac{\partial M}{\partial \mu} \right) \right\rangle \right] + \dots \end{aligned} \quad (42)$$

$$\begin{aligned} &= \langle \mathcal{O} \rangle + \mu \alpha N_f \left\langle \mathcal{O} \overline{\left( \eta^\dagger M^{-1} \frac{\partial M}{\partial \mu} \eta \right)} \right\rangle \\ &+ \frac{\mu^2}{2} (\alpha N_f)^2 \left[ \left\langle \mathcal{O} \overline{\left( \eta^\dagger M^{-1} \frac{\partial M}{\partial \mu} \eta \right)}^2 \right\rangle - \left\langle \mathcal{O} \varepsilon^2 \left( M^{-1} \frac{\partial M}{\partial \mu} \right) \right\rangle \right] \\ &+ \frac{\mu^2}{2} \alpha N_f \left[ \left\langle \mathcal{O} \overline{\left( \eta^\dagger M^{-1} \frac{\partial^2 M}{\partial \mu^2} \eta \right)} \right\rangle - \left\langle \mathcal{O} \overline{\left( \eta^\dagger M^{-1} \frac{\partial M}{\partial \mu} M^{-1} \frac{\partial M}{\partial \mu} \eta \right)} \right\rangle \right] + \dots \end{aligned} \quad (43)$$

$$\begin{aligned} &= \left\langle \mathcal{O} \exp \left\{ \mu \alpha N_f \overline{\left( \eta^\dagger M^{-1} \frac{\partial M}{\partial \mu} \eta \right)} \right. \right. \\ &\quad \left. \left. - \frac{\mu^2}{2} (\alpha N_f)^2 \varepsilon^2 \left( M^{-1} \frac{\partial M}{\partial \mu} \right) + \frac{\mu^2}{2} \alpha N_f \left[ \overline{\left( \eta^\dagger M^{-1} \frac{\partial^2 M}{\partial \mu^2} \eta \right)} - \overline{\left( \eta^\dagger M^{-1} \frac{\partial M}{\partial \mu} M^{-1} \frac{\partial M}{\partial \mu} \eta \right)} \right] + \dots \right\} \right\rangle, \end{aligned} \quad (44)$$

where  $\overline{(\dots)}$  denotes the average over the noise vectors. The denominator of eqn.(2) is given by the same expression with  $\mathcal{O} = 1$ . In each case a term proportional to  $\varepsilon^2$  appears. In Fig. 25, we estimate the effect of this term by subtracting this term from original one. The difference for  $\chi_L$  by the subtraction is found to be quite small, e.g., that is less than 1% at  $m = 0.2$  and  $\mu \leq 0.1$ . The result suggests the contribution from the term of  $\varepsilon^2$  is small for  $\chi_L$  although the value of  $\varepsilon[M^{-1}(\partial M/\partial \mu)]^2$  itself is not small.

For the case of a fermionic operator such as  $\bar{\psi} \psi$  many such additional terms appear in the reweighting formula. In this study, we neglect the effect from further additional terms, since Fig. 25 suggests that the effect is small for the determination of  $\beta_c$ .

TABLE I. Simulation point  $(m, \beta)$  and number of configurations  $N_{\text{conf}}$  for mass-reweighting and  $\mu$ -reweighting.

| $m$ | $\beta$ | $N_{\text{conf}}(\text{mass})$ | $N_{\text{conf}}(\mu)$ |
|-----|---------|--------------------------------|------------------------|
| 0.1 | 3.640   | 38000                          | 20000                  |
|     | 3.645   | 15000                          |                        |
|     | 3.650   | 58000                          | 38000                  |
|     | 3.655   | 16800                          |                        |
|     | 3.660   | 55000                          | 40000                  |
|     | 3.665   | 7800                           |                        |
|     | 3.670   | 30000                          | 30000                  |
| 0.2 | 3.740   | 5000                           |                        |
|     | 3.750   | 30000                          | 20000                  |
|     | 3.755   | 15000                          |                        |
|     | 3.760   | 52000                          | 34000                  |
|     | 3.770   | 48000                          | 32000                  |
|     | 3.780   | 5000                           |                        |

TABLE II. Quark mass dependence of transition point determined by  $L$  and  $\langle\bar{\psi}\psi\rangle$ . The fitting function is  $\beta_c = \beta_c(m_0) + \sum_{n=1}^{N_{\text{fit}}} c_i(m - m_0)^n$ . The truncation error is contained in  $c_2$  from  $\bar{\psi}\psi$ .

|                  | $m_0$ | $\beta_c(m_0)$ | $c_1$      | $c_2$      | fit range                  | $N_{\text{fit}}$ |
|------------------|-------|----------------|------------|------------|----------------------------|------------------|
| $\bar{\psi}\psi$ | 0.1   | 3.6492(22)     | 1.05(14)   | -          | $-0.01 < m - m_0 < 0.01$   | 1                |
|                  |       | 3.6492(22)     | 1.03(13)   | [-9.(14)]  | $-0.01 < m - m_0 < 0.01$   | 2                |
|                  |       | 3.6492(22)     | 1.07(19)   | -          | $-0.005 < m - m_0 < 0.005$ | 1                |
|                  |       | 3.6492(22)     | 1.07(19)   | [-17.(26)] | $-0.005 < m - m_0 < 0.005$ | 2                |
|                  | 0.2   | 3.7617(36)     | 0.896(90)  | -          | $-0.02 < m - m_0 < 0.02$   | 1                |
|                  |       | 3.7617(36)     | 0.894(89)  | [5.(13)]   | $-0.02 < m - m_0 < 0.02$   | 2                |
|                  |       | 3.7617(36)     | 0.970(168) | -          | $-0.01 < m - m_0 < 0.01$   | 1                |
|                  |       | 3.7617(36)     | 0.999(180) | [18.(39)]  | $-0.01 < m - m_0 < 0.01$   | 2                |
| Polyakov         | 0.2   | 3.7639(19)     | 0.838(64)  | -          | $-0.02 < m - m_0 < 0.02$   | 1                |
|                  |       | 3.7639(19)     | 0.835(63)  | -2.7(4.5)  | $-0.02 < m - m_0 < 0.02$   | 2                |
|                  |       | 3.7639(19)     | 0.883(106) | -          | $-0.01 < m - m_0 < 0.01$   | 1                |
|                  |       | 3.7639(19)     | 0.885(106) | -4.7(10.0) | $-0.01 < m - m_0 < 0.01$   | 2                |

TABLE III.  $\beta_c$  and its second derivative with respect to  $\mu$ . We fit the data with the function  $\beta_c(\mu) = \beta_c(0) + \sum_{n=1}^{N_{\text{fit}}} c_n \mu^{2n}$ , where  $d^2\beta_c/d\mu^2 = 2c_1$ .

|                  | $m$ | $\beta_c$  | $d^2\beta_c/d\mu^2$ | fit range                 | $N_{\text{fit}}$ |
|------------------|-----|------------|---------------------|---------------------------|------------------|
| $\bar{\psi}\psi$ | 0.1 | 3.6497(16) | -1.20(44)           | $0 \leq \mu^2 \leq 0.008$ | 1                |
|                  |     | 3.6497(16) | -1.19(54)           | $0 \leq \mu^2 \leq 0.005$ | 1                |
|                  |     | 3.6497(16) | -1.21(79)           | $0 \leq \mu^2 \leq 0.008$ | 2                |
|                  |     | 3.7641(37) | -1.02(56)           | $0 \leq \mu^2 \leq 0.014$ | 1                |
|                  | 0.2 | 3.7641(37) | -1.10(68)           | $0 \leq \mu^2 \leq 0.010$ | 1                |
|                  |     | 3.7641(37) | -1.34(103)          | $0 \leq \mu^2 \leq 0.014$ | 2                |
|                  |     | 3.7651(16) | -1.01(23)           | $0 \leq \mu^2 \leq 0.014$ | 1                |
| Polyakov         | 0.2 | 3.7651(16) | -1.07(24)           | $0 \leq \mu^2 \leq 0.010$ | 1                |
|                  |     | 3.7651(16) | -1.21(31)           | $0 \leq \mu^2 \leq 0.014$ | 2                |

TABLE IV. Average of  $\langle \text{Im} \text{tr}[(\partial M/\partial \mu)M^{-1}] \rangle$ , average of its error for each configuration ( $\langle \varepsilon \rangle$ ), standard deviation (STD) and improved standard deviation (STD(Imp.)).

| $m$ | $\beta$ | $\langle \text{Im} \text{tr}[(\partial M/\partial \mu)M^{-1}] \rangle$ | $\langle \varepsilon \rangle$ | STD     | STD(Imp.) |
|-----|---------|--|-------------------------------|---------|-----------|
| 0.1 | 3.64    | $-1.15 \times 10^{-4}$   | 0.00199                       | 0.00233 | 0.00110   |
|     | 3.65    | $1.02 \times 10^{-5}$  | 0.00194                       | 0.00223 | 0.00099   |
|     | 3.66    | $-3.06 \times 10^{-5}$   | 0.00189                       | 0.00212 | 0.00085   |
|     | 3.67    | $-1.40 \times 10^{-5}$   | 0.00185                       | 0.00206 | 0.00077   |
| 0.2 | 3.75    | $1.03 \times 10^{-5}$  | 0.00141                       | 0.00168 | 0.00085   |
|     | 3.76    | $0.93 \times 10^{-5}$  | 0.00140                       | 0.00161 | 0.00072   |
|     | 3.77    | $-4.17 \times 10^{-5}$   | 0.00138                       | 0.00155 | 0.00061   |

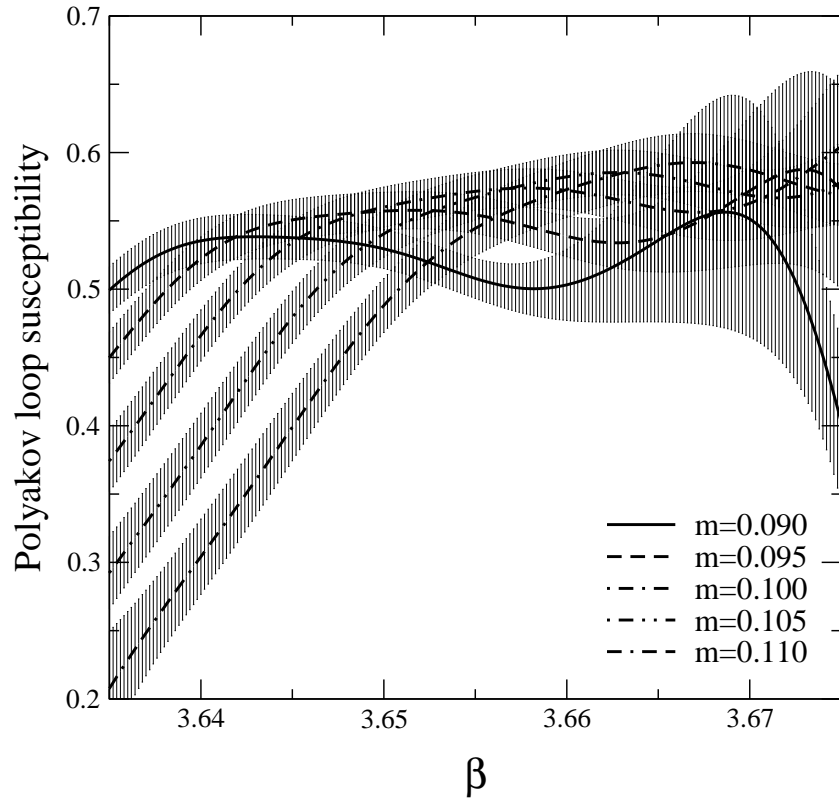


FIG. 1. Quark mass dependence of  $\chi_L$  as a function of  $\beta$  at  $m_0 = 0.1$ .

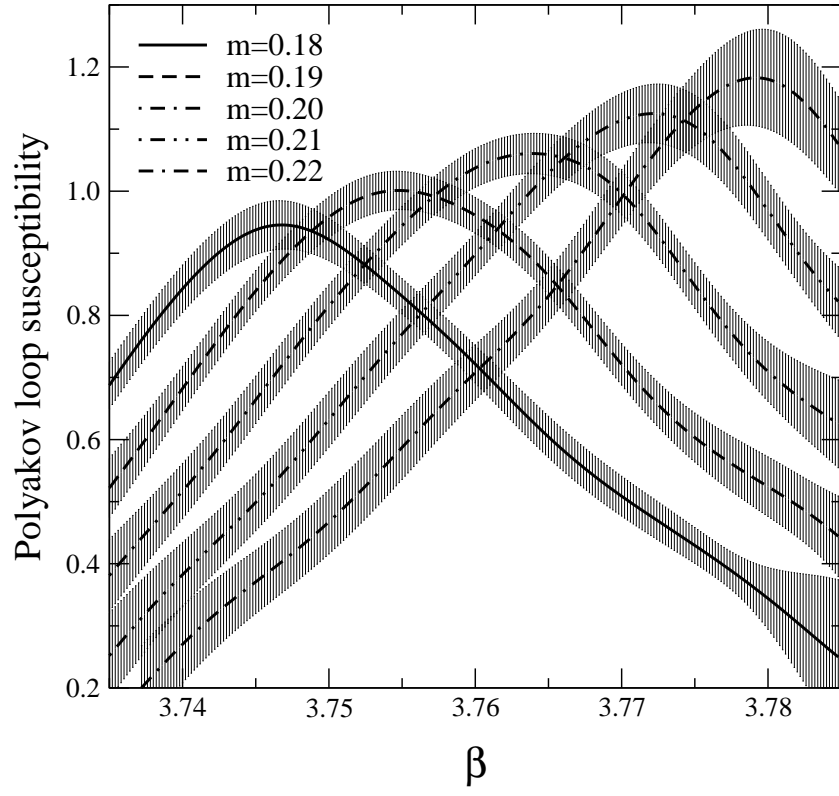


FIG. 2. Quark mass dependence of  $\chi_L$  as a function of  $\beta$  at  $m_0 = 0.2$ .

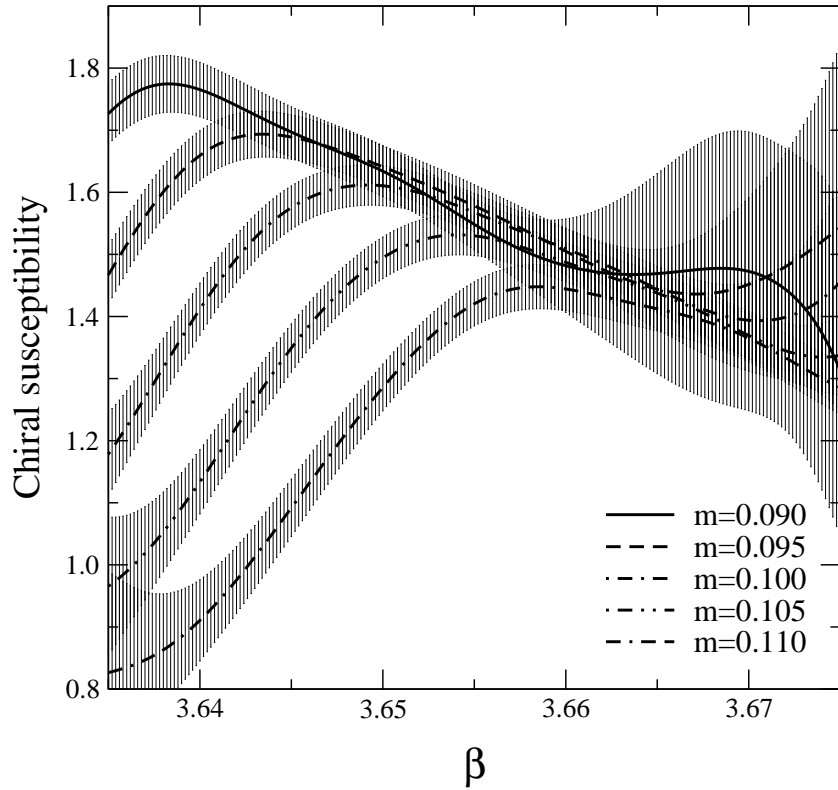


FIG. 3. Quark mass dependence of  $\chi_{\bar{\psi}\psi}$  as a function of  $\beta$  at  $m_0 = 0.1$ .

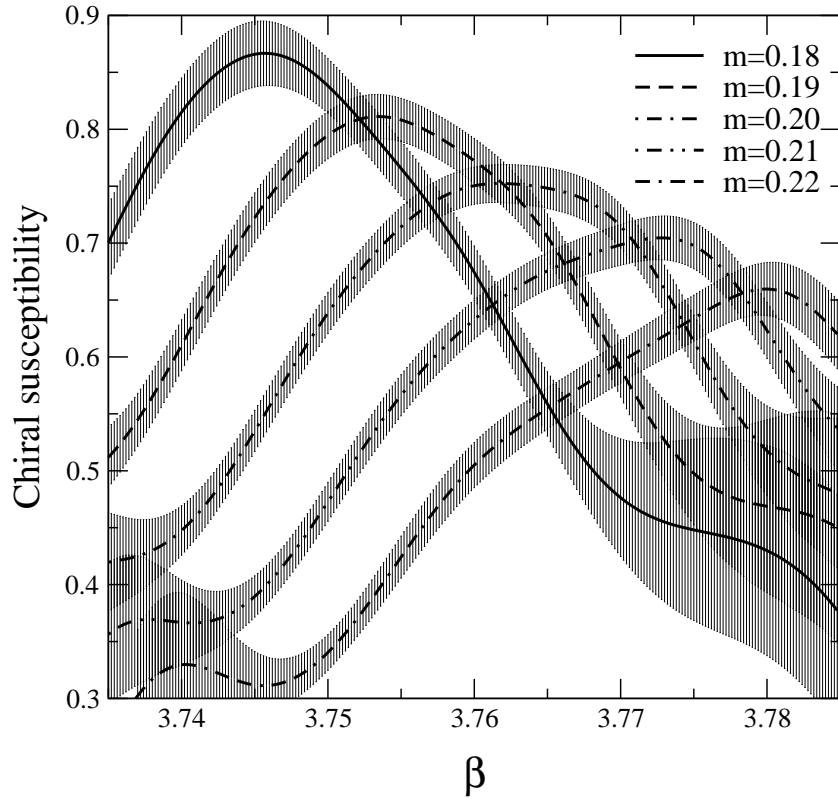


FIG. 4. Quark mass dependence of  $\chi_{\bar{\psi}\psi}$  as a function of  $\beta$  at  $m_0 = 0.2$ .

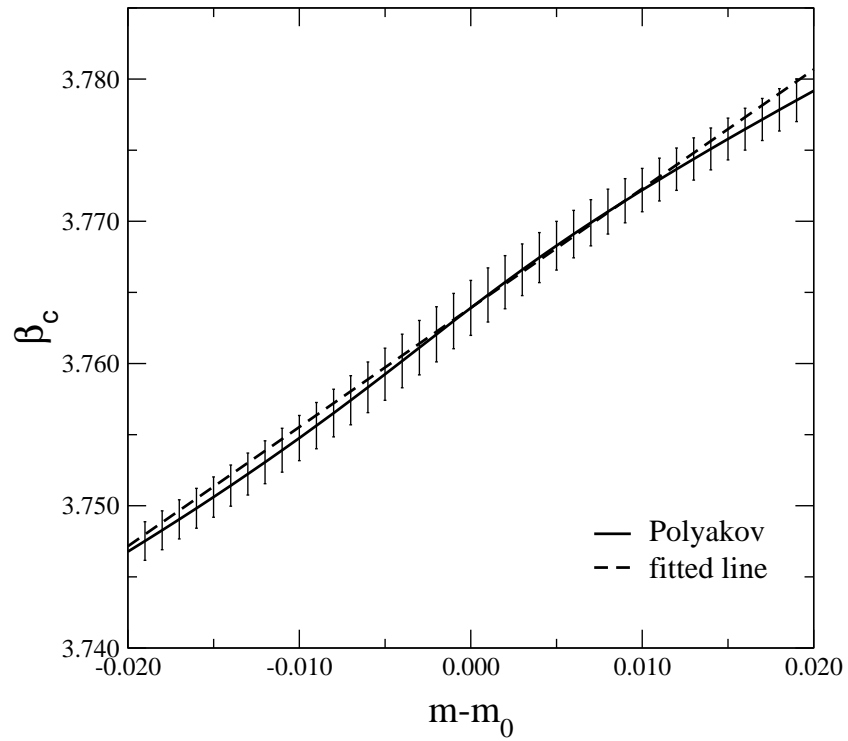


FIG. 5.  $\beta_c(m)$  determined by  $\chi_L$  around  $m_0 = 0.2$ .

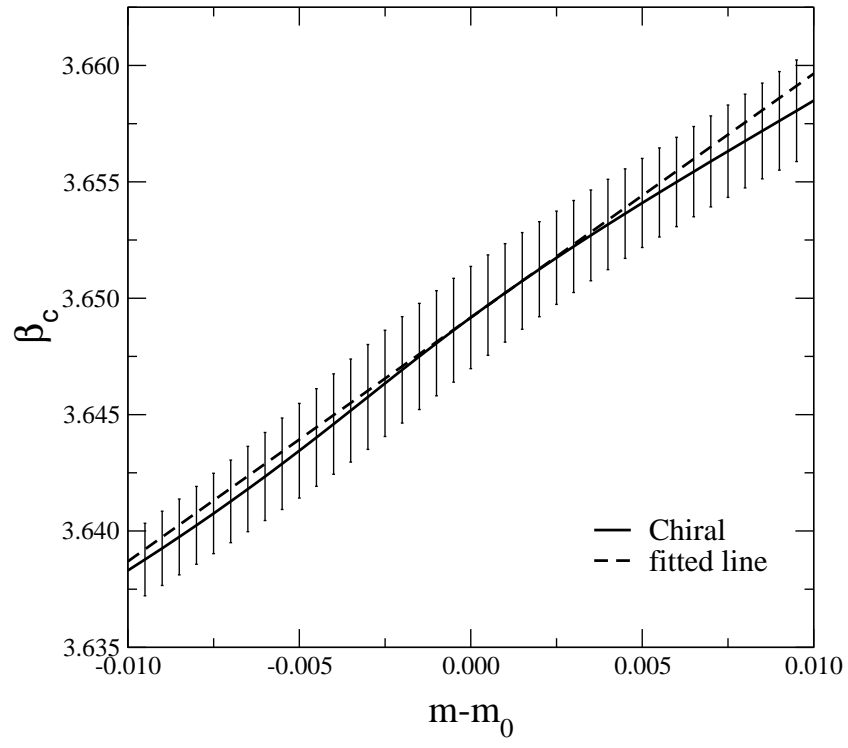


FIG. 6.  $\beta_c(m)$  determined by  $\chi_{\bar{\psi}\psi}$  around  $m_0 = 0.1$ .

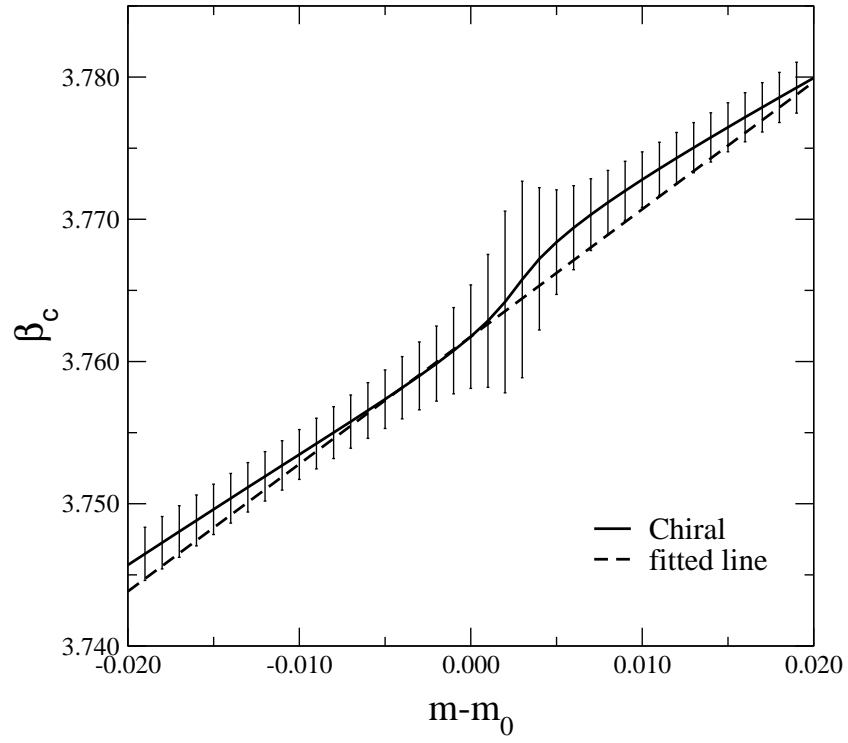


FIG. 7.  $\beta_c(m)$  determined by  $\chi_{\bar{\psi}\psi}$  around  $m_0 = 0.2$ .

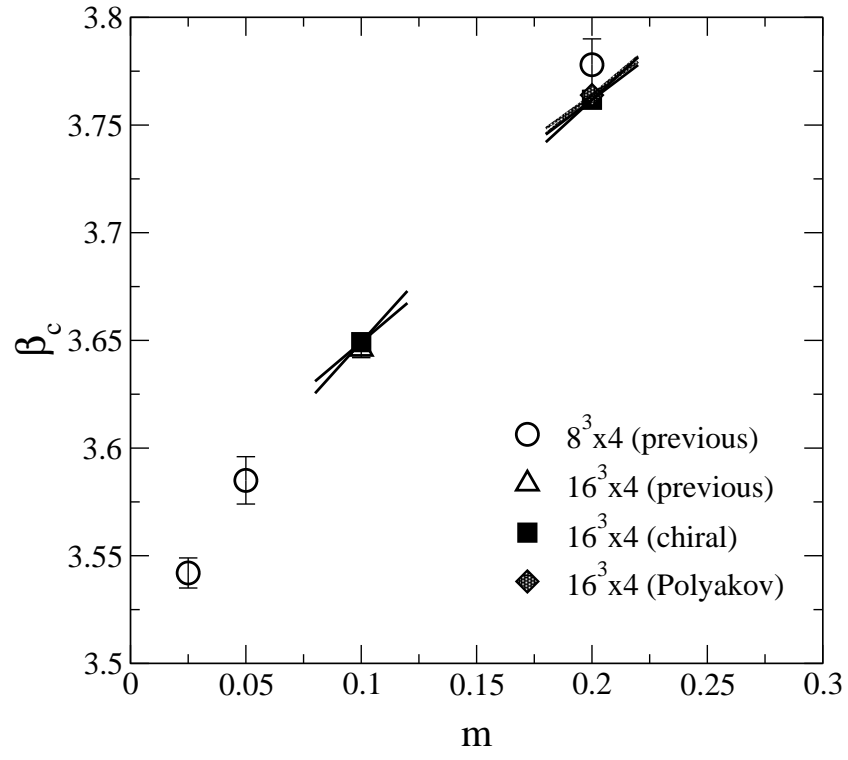


FIG. 8.  $\beta_c(m)$  determined by  $\chi_{\bar{\psi}\psi}$  in comparison with previous results.

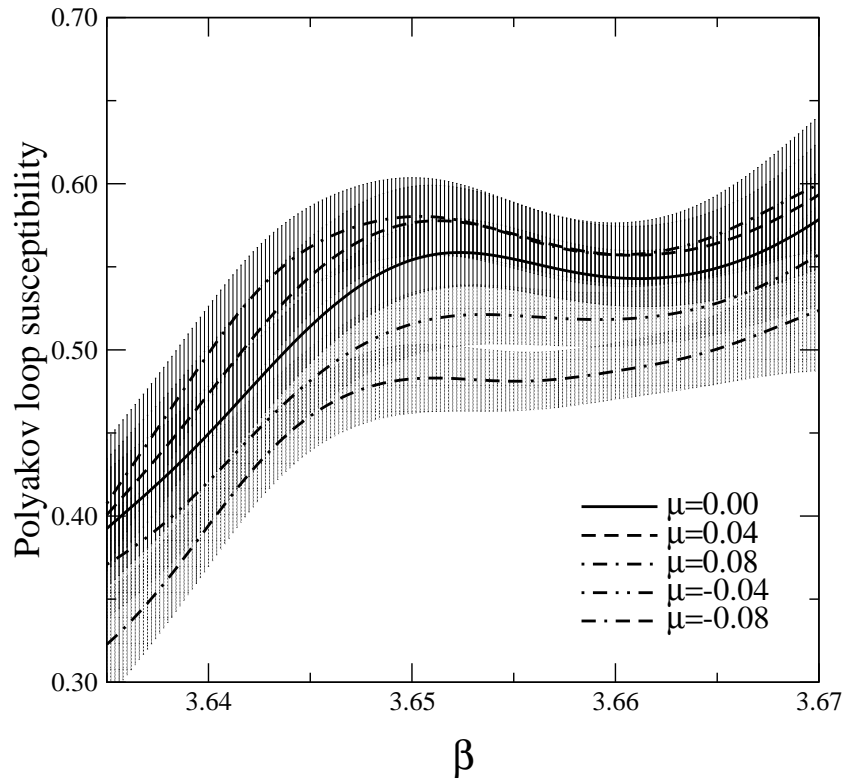


FIG. 9.  $\chi_L(\beta)$  at  $m = 0.1$  for various  $\mu$ .

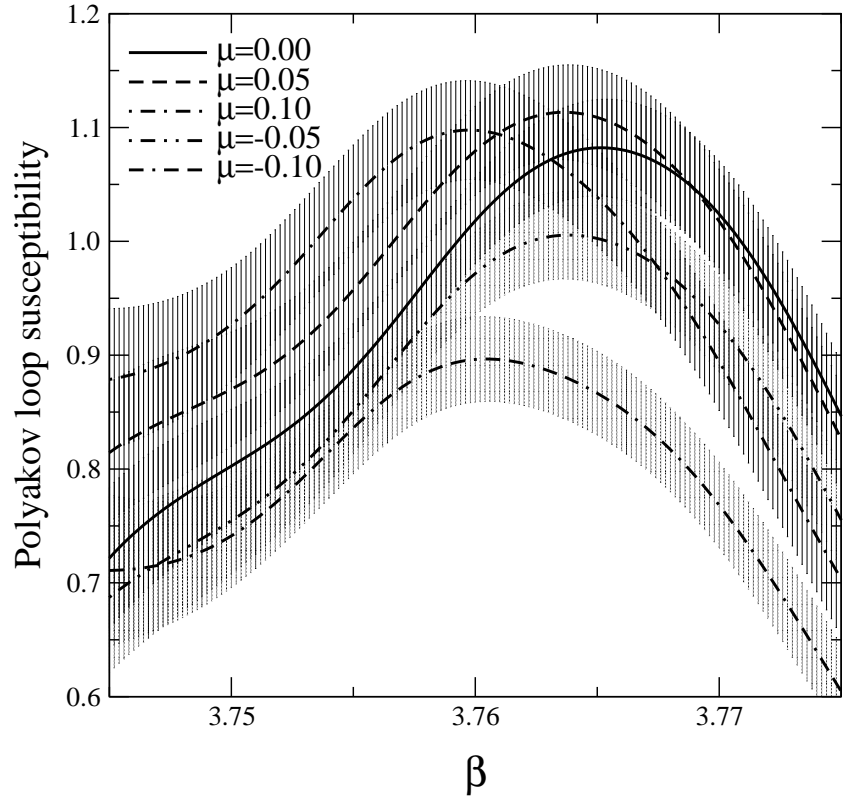


FIG. 10.  $\chi_L(\beta)$  at  $m = 0.2$  for various  $\mu$ .

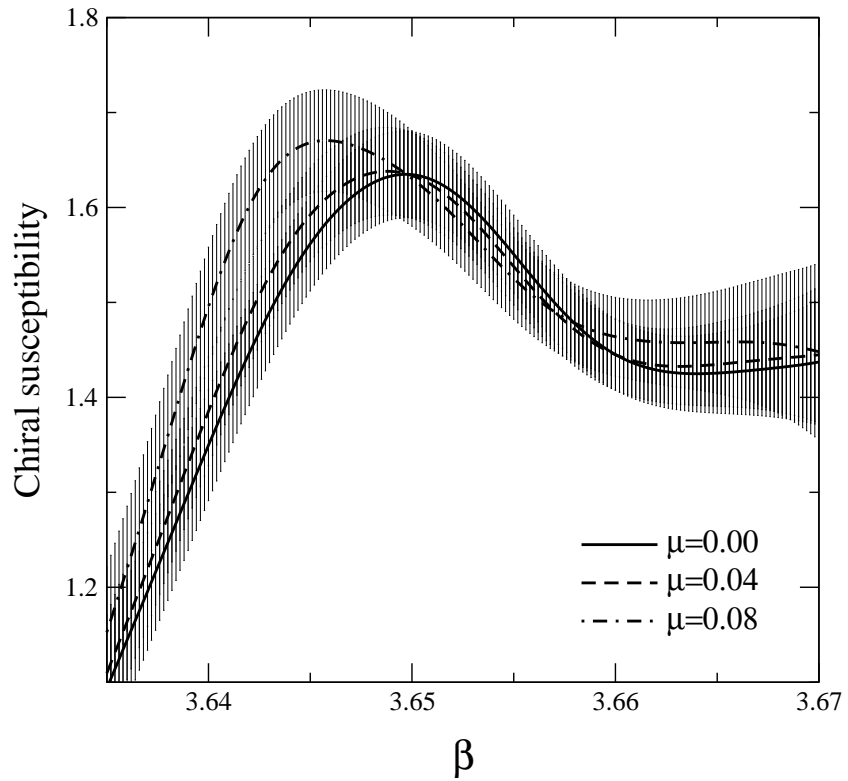


FIG. 11.  $\chi_{\bar{\psi}\psi}(\beta)$  at  $m = 0.1$  for various  $\mu$ .

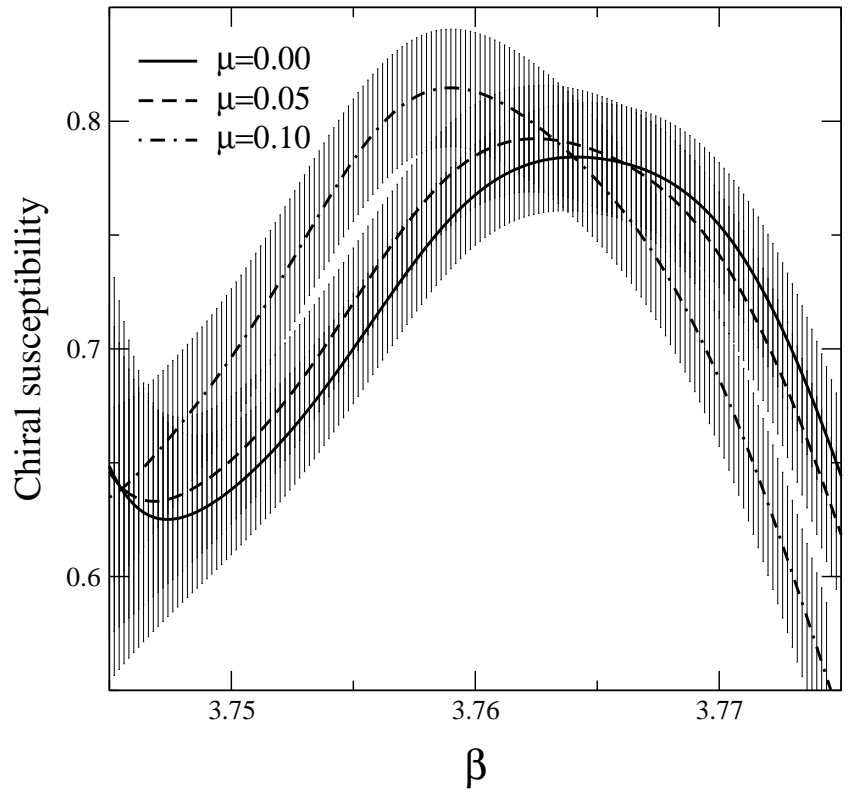


FIG. 12.  $\chi_{\bar{\psi}\psi}(\beta)$  at  $m = 0.2$  for various  $\mu$ .

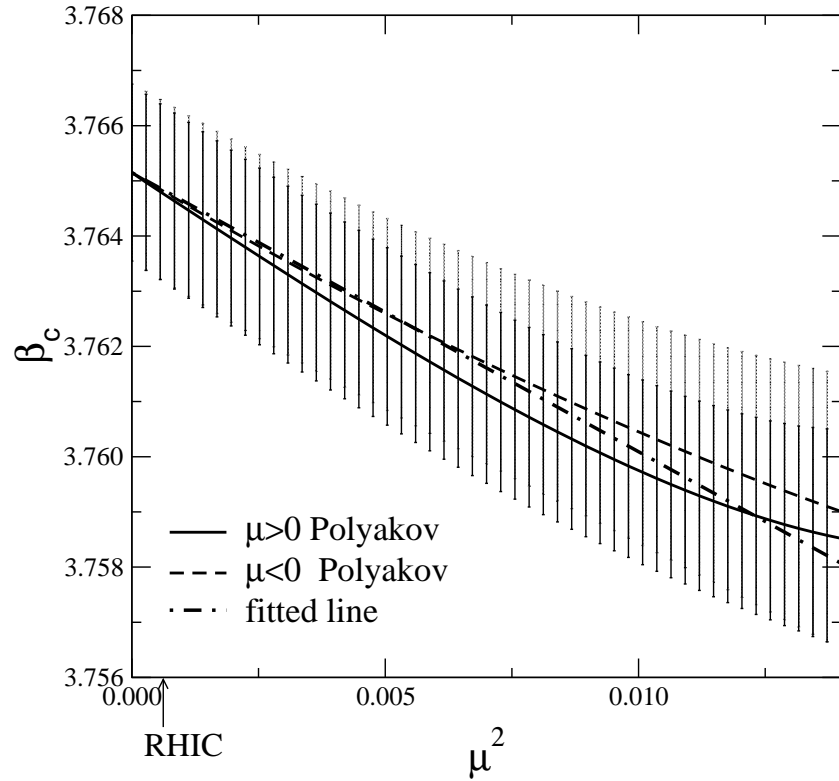


FIG. 13. Phase transition point  $\beta_c(\mu)$  determined by  $\chi_L$  at  $m = 0.2$ .

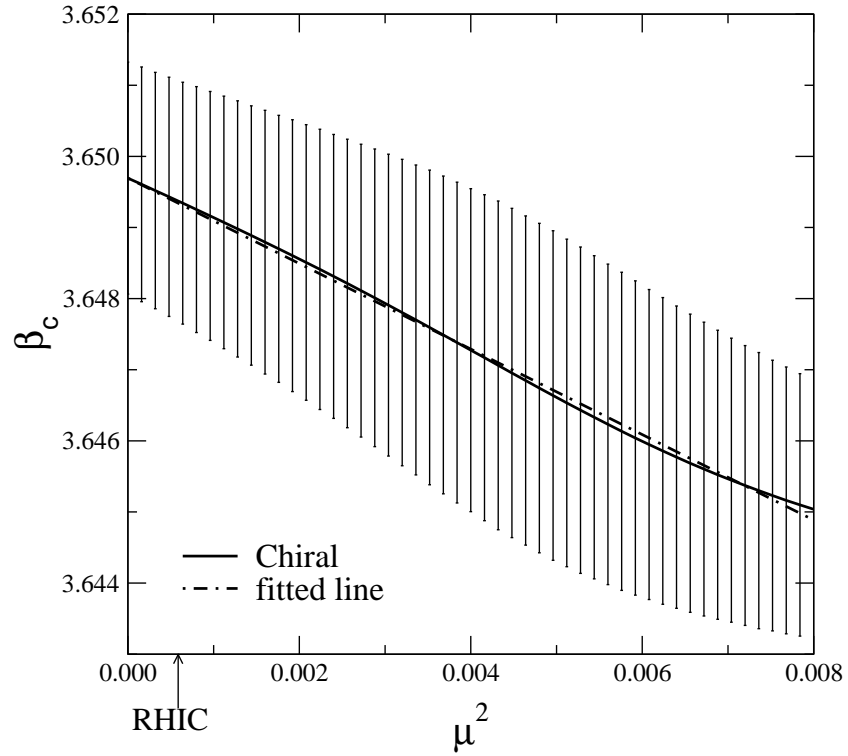


FIG. 14. Phase transition point  $\beta_c(\mu)$  determined by  $\chi_{\bar{\psi}\psi}$  at  $m = 0.1$ .

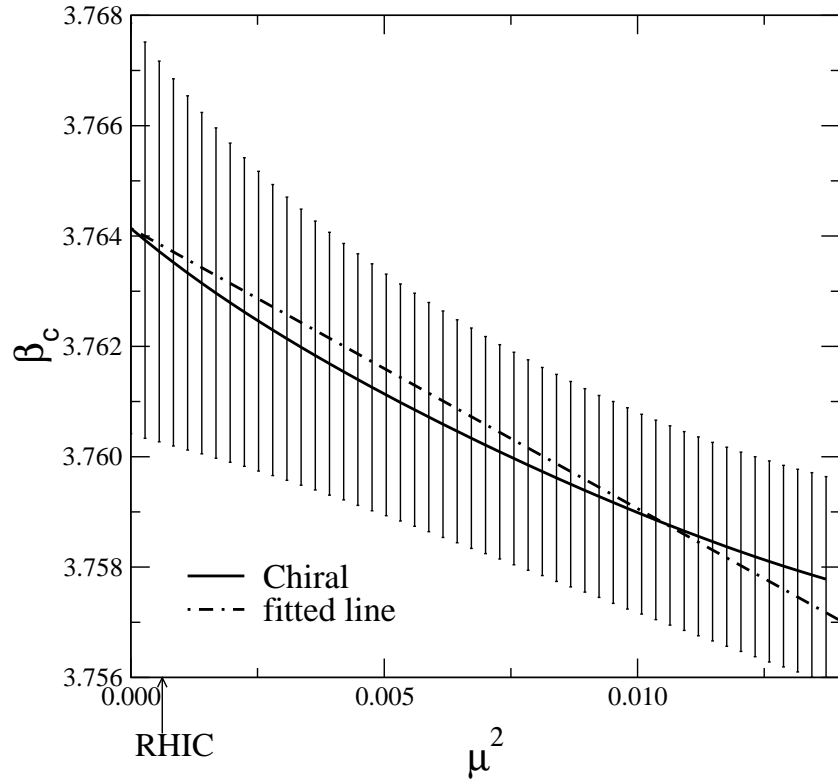


FIG. 15. Phase transition point  $\beta_c(\mu)$  determined by  $\chi_{\bar{\psi}\psi}$  at  $m = 0.2$ .

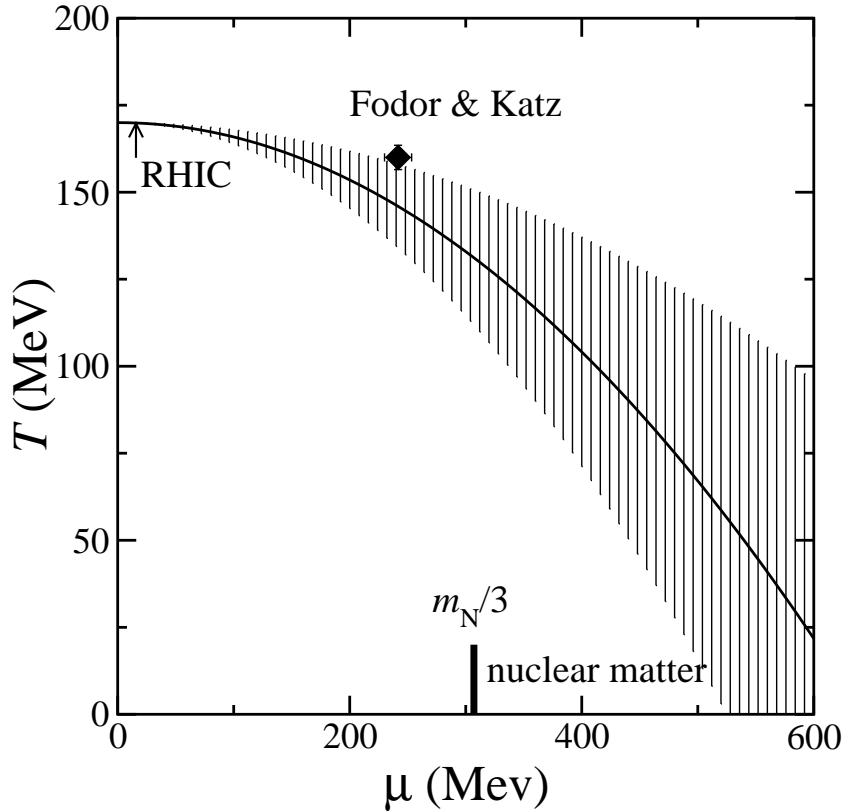


FIG. 16. Sketch of the phase diagram, as estimated using our value of the curvature of  $\beta_c(\mu = 0)$ . The diamond symbol is the end point of the first order phase transition obtained by Fodor and Katz [7].

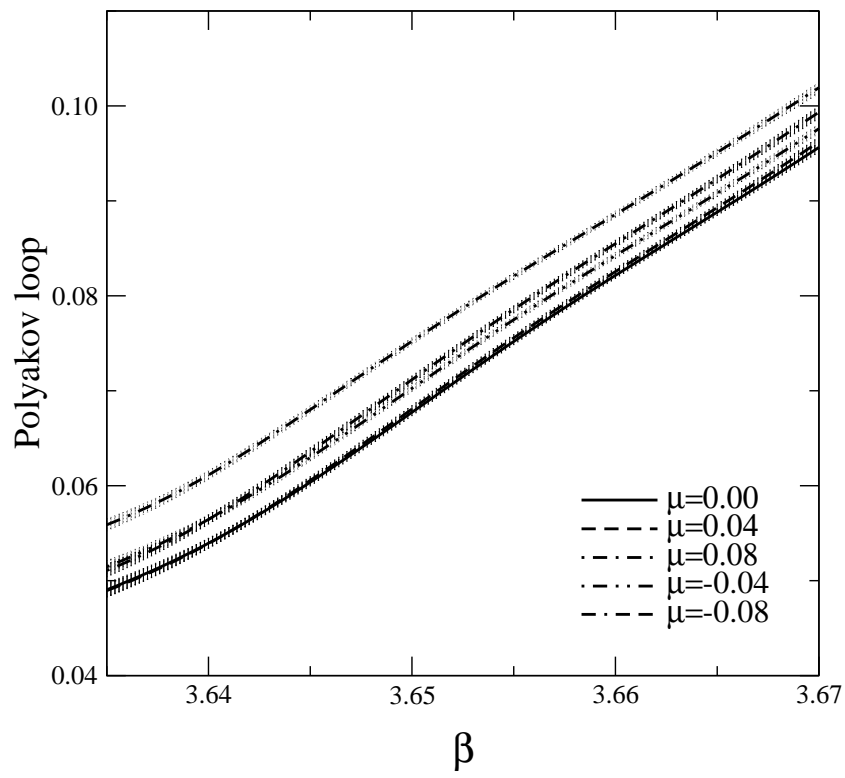


FIG. 17.  $L(\beta)$  at  $m = 0.1$  for various  $\mu$ .

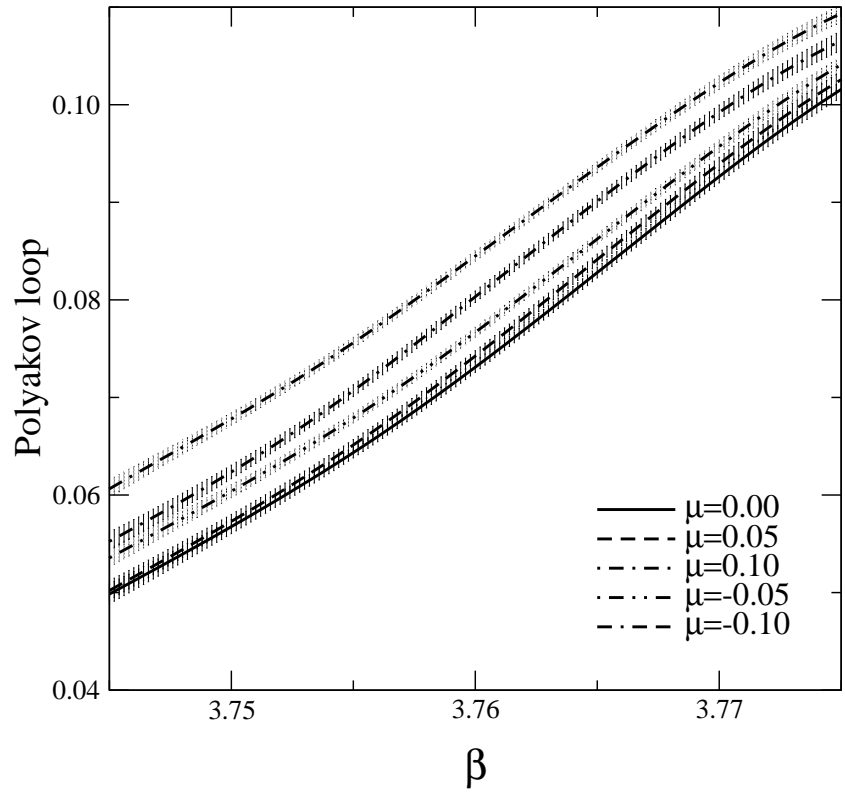


FIG. 18.  $L(\beta)$  at  $m = 0.2$  for various  $\mu$ .

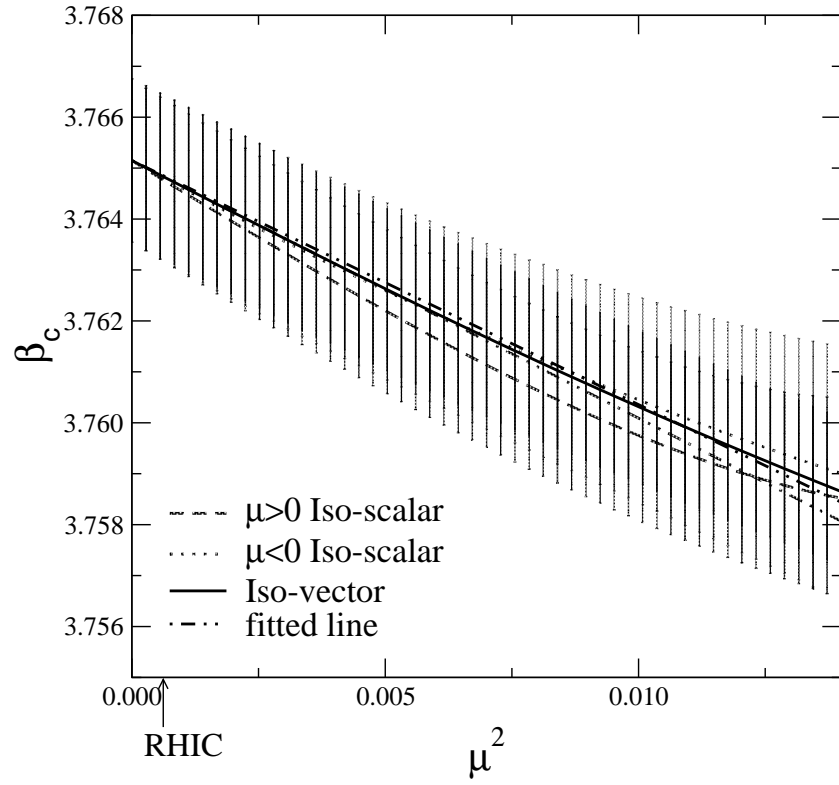


FIG. 19. Difference between  $\mu$  and  $\mu_I$  for  $\beta_c$  determined by  $\chi_L$  at  $m = 0.2$ .

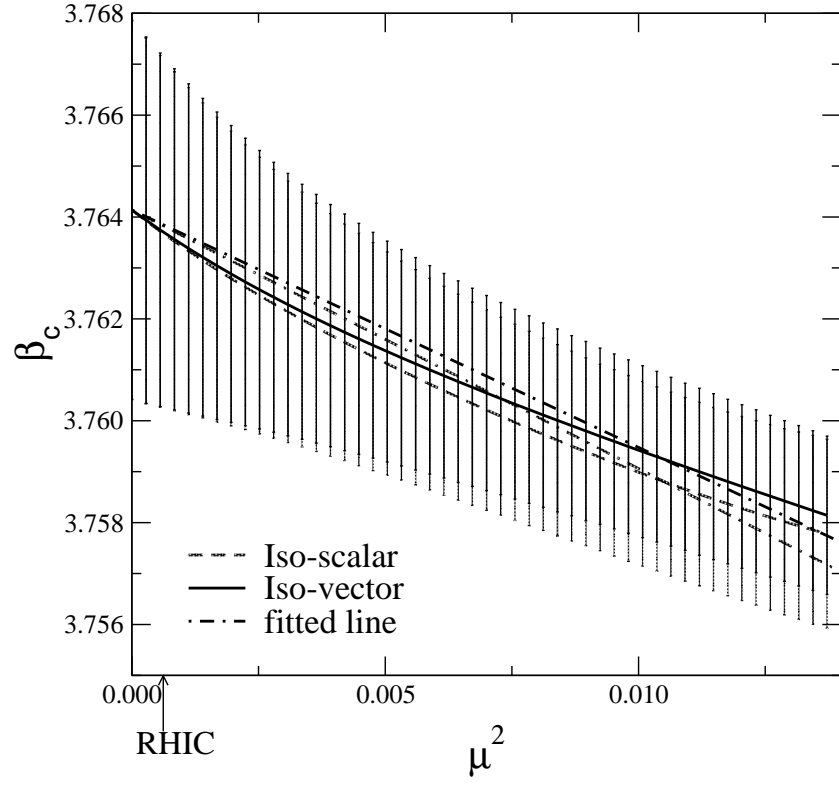


FIG. 20. Difference between  $\mu$  and  $\mu_I$  for  $\beta_c$  determined by  $\chi_{\bar{\psi}\psi}$  at  $m = 0.2$ .

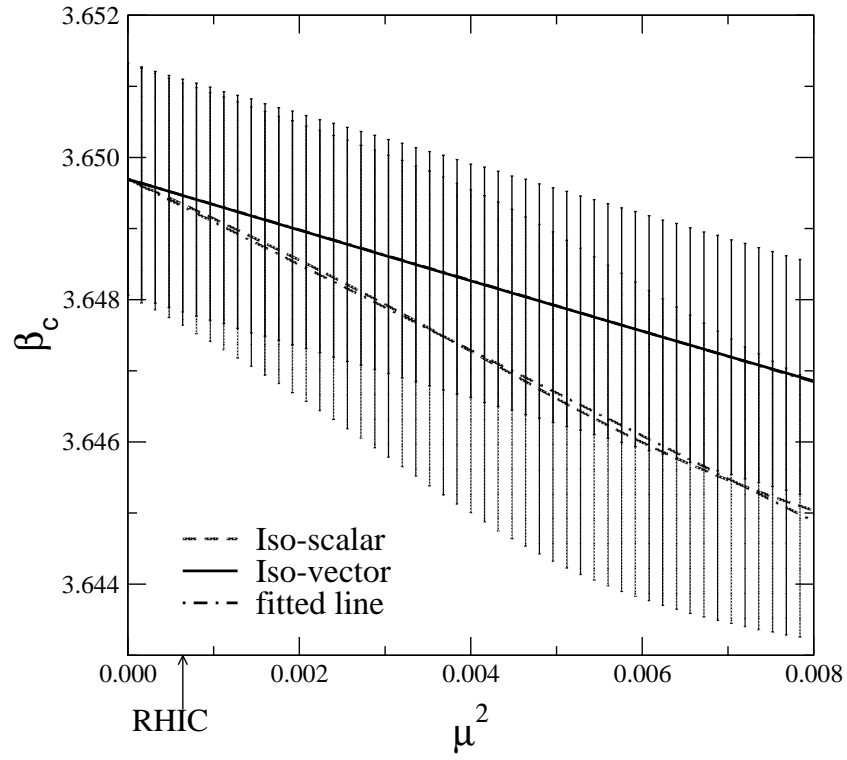


FIG. 21. Difference between  $\mu$  and  $\mu_I$  for  $\beta_c$  determined by  $\chi_{\bar{\psi}\psi}$  at  $m = 0.1$ .

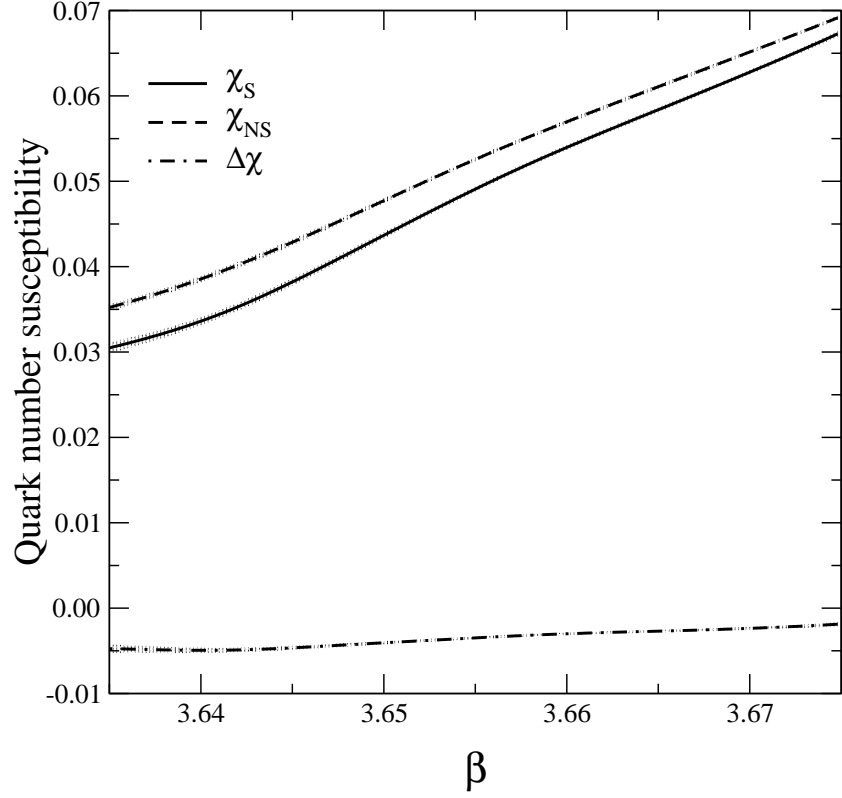


FIG. 22. Quark number susceptibilities  $\chi_S$  and  $\chi_{NS}$  at  $m = 0.1$ .  $\Delta\chi = \chi_S - \chi_{NS}$ .

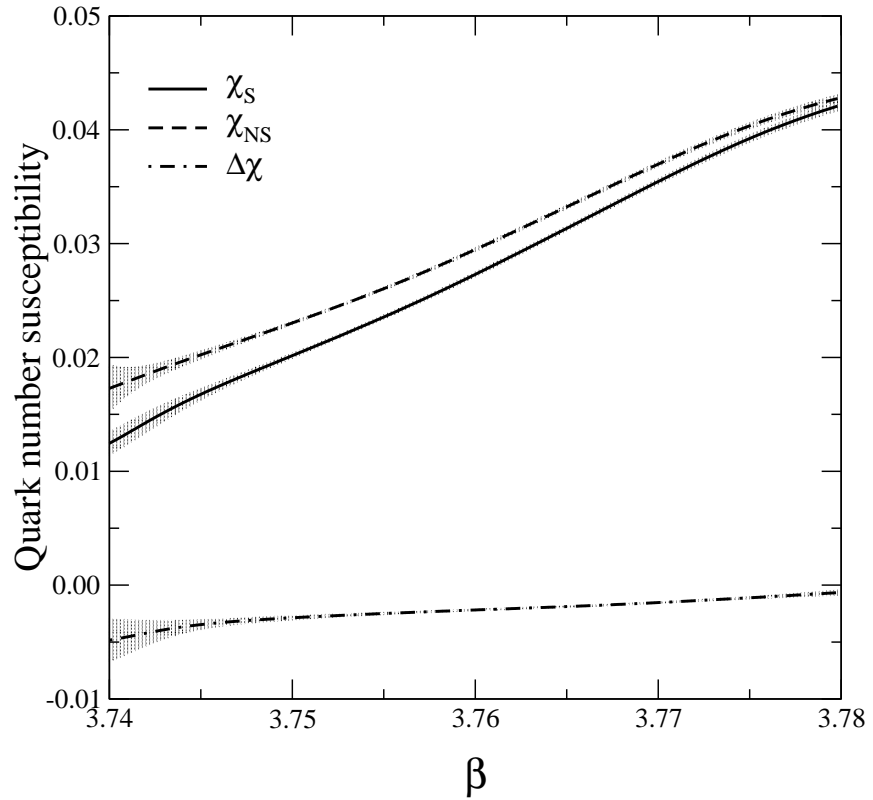


FIG. 23. Quark number susceptibilities  $\chi_S$  and  $\chi_{NS}$  at  $m = 0.2$ .

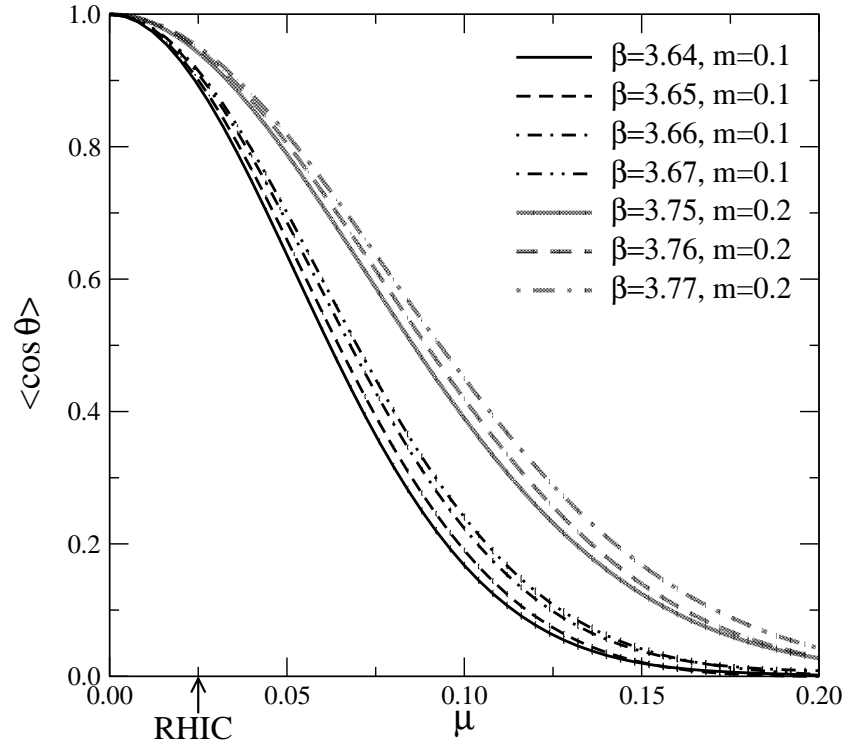


FIG. 24. The expectation value of the complex phase  $\langle \cos \theta \rangle$ .

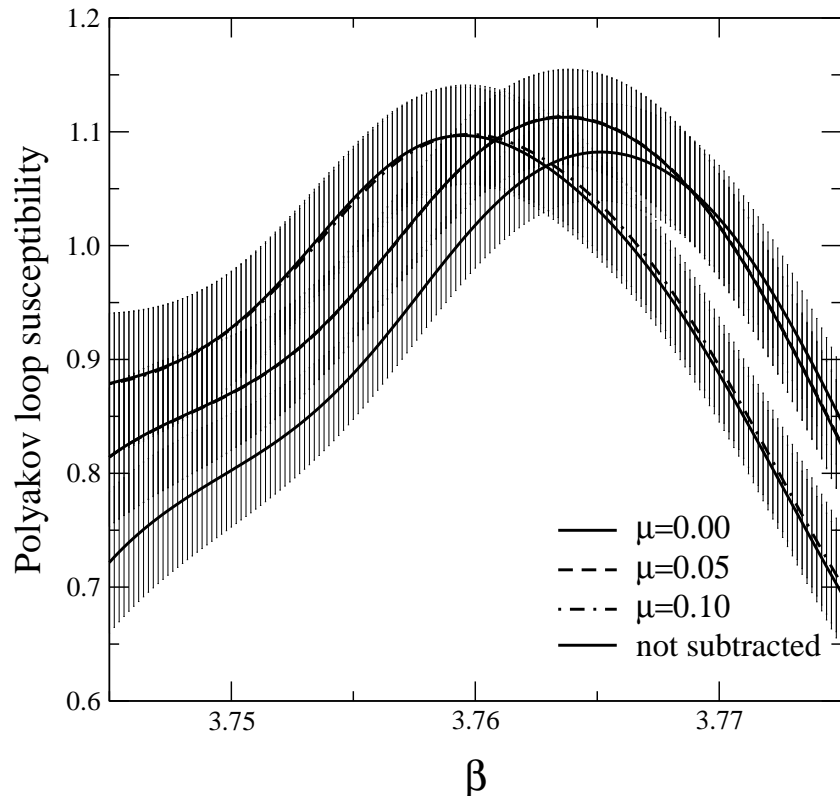


FIG. 25. Effect from the term of  $O(\varepsilon^2)$  on  $\chi_L$  at  $m = 0.2$ . Solid lines are the same as Fig. 10 obtained including the  $O(\varepsilon^2)$  term, and dashed lines are calculated without it.